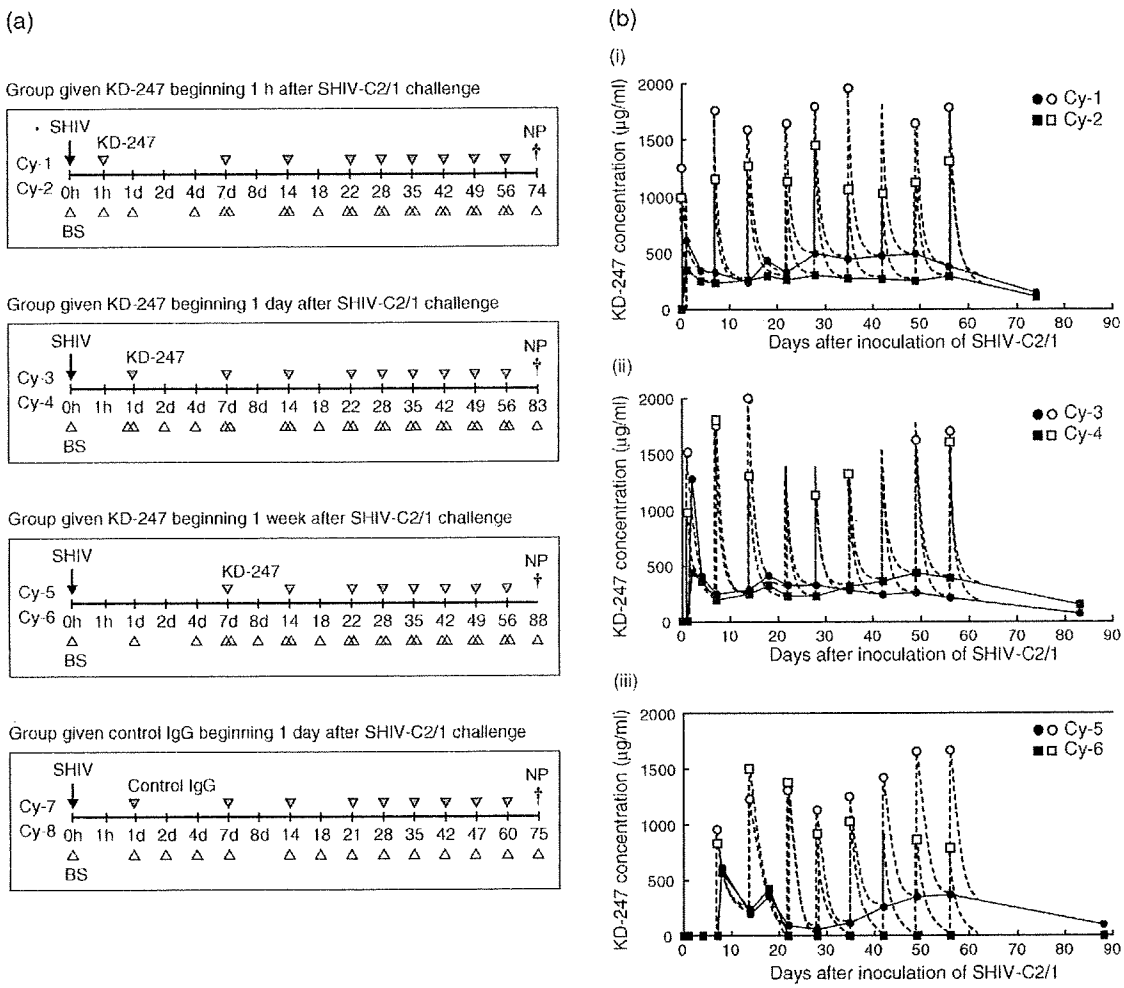

Fig. 1. KD-247 administration schedules and pharmacokinetic profiles. (a) Scheme of viral challenge and postinfection passive immunization with KD-247. A total of eight cynomolgus monkeys were used for viral infection studies with highly pathogenic SHIV-C2/1 (20 $TCID_{50}$). In the first group of two monkeys, 45 mg/kg of KD-247 was intravenously administered at 1 h after viral challenge and antibody administered once per week for 2 months. Monkeys in the second and third groups were injected with antibody at 1 day and 1 week after viral challenge, respectively, and similarly treated with the antibody. Monkeys in the fourth group were injected with 45 mg/kg of human normal immunoglobulin fraction at 1 day after viral challenge followed by passive transfer of this control IgG once a week for 2 months. Two other monkeys were used as positive controls for infection by SHIV-C2/1 with 20 $TCID_{50}$ without passive transfer of antibody, whereas 15 other monkeys were used as naive controls without viral infection and antibody transfer. (b) KD-247 concentrations in the plasma of monkeys treated 1 h (i), 1 day (ii), or 1 week (iii) after SHIV-C2/1 challenge. Closed and open symbols indicate KD-247 concentrations in plasma collected immediately before and 15 min after administration of KD-247, respectively. Broken lines show the estimated changes in KD-247 concentrations. BS, blood sampling; NP, necropsy; SHIV-C2/1, simian/human immunodeficiency virus C2/1; $TCID_{50}$, 50% tissue culture infective dose.

stopped. The plates were measured for optical density at 450 nm with a precision microplate reader (Emax; Molecular Devices, Menlo Park, California, USA). The concentrations of KD-247 antibody in the plasma were evaluated from a calibration curve drawn with software developed for the reader (SOFTmax; Molecular Devices).

Detection of anti-KD-247 antibodies

Anti-KD-247 antibodies in plasma were detected using 96-well ELISA plates (MaxiSorp) coated with KD-247. After washing and blocking, samples containing test monkey plasma at 1 : 400 dilution or a positive control were then added and incubated. A positive control was pooled with rabbit anti-KD-247 plasma at 1 : 4000 dilution. The wells were washed, incubated with biotinylated KD-247, and then washed again. Peroxidase-conjugated streptavidin (Sigma Chemical, St. Louis, Missouri, USA) was diluted and added to the wells for reaction.

Real-time reverse transcriptase-PCR quantitation of simian/human immunodeficiency virus RNA in plasma

Plasma viral loads were evaluated by real-time reverse transcriptase PCR (RT-PCR) as described previously

[17,18]. Viral RNA in plasma was extracted and purified using the QIAamp Viral RNA Mini Kit (Qiagen, Valencia, California, USA). For quantitative analysis of the RNA,. the TaqMan system (Applied Biosystems, Foster City, California, USA) was used with primers and probes targeting the SIVmac239 *gag* region. The viral RNA was amplified using TaqMan EZ RT-PCR Kit (Applied Biosystems) with primers. The RT-PCR product was quantitatively monitored by its fluorescent intensity with ABI7700 (Applied Biosystems). Plasma viral load, which was measured in duplicate, was calculated based on the standard curve of control RNA and RNA recovery rate. The limit of detection was approximately 500 RNA copies/ml.

Flow cytometric evaluation of cell surface antigen expression and absolute cell count

Lymphoid cells for flow cytometric analyses were prepared from intact thymuses, spleens, and lymph nodes. Mouse mAbs conjugated with either fluorescein isothiocyanate (FITC), phycoerythrin, phycoerythrin-Cy5, or peridinin chlorophyll protein (PerCP) were used in flow cytometric analyses to detect cellular expression of monkey CD3 (NF-18; BioSource International, Camarillo, California, USA), human CD4 (SK3; Becton Dickinson, San Jose, California, USA), and CD8 (SK1; Becton Dickinson). To determine absolute cell counts, samples of whole blood were analyzed following the addition of FITC-conjugated anti-CD3 (BioSource), phycoerythrin-conjugated anti-CD4 (Becton Dickinson), and PerCP-conjugated anti-CD8 mAbs (Becton Dickinson), as previously described [19].

Results

KD-247 concentrations and detection of anti-KD-247 antibodies in monkey plasma

Blood was drawn from monkeys before and after the administration of KD-247 and at necropsy (Fig. 1a). In the monkeys that were given antibody beginning 1 h (Cy-1 and Cy-2) or 1 day (Cy-3 and Cy-4) after challenge with SHIV-C2/1, concentrations of KD-247 peaked at 800–2000 μg/ml at 15 min after injection and were maintained at 200–500 μg/ml until the next administration (as evidenced in blood samples drawn before each administration and within 15 min of the injection) (Fig. 1b i and ii). The plasma concentrations of KD-247 in monkeys treated beginning 1 week after challenge with the virus (Cy-5 and Cy-6) did not remain constant. In particular, the KD-247 maintenance concentrations in Cy-6 after day 22 were below the limit of detection (2.5 μg/ml) of the assay (Fig. 1b iii).

Because KD-247 was repeatedly administered to the monkeys, we also considered the possibility of anti-KD-247 antibody production. Anti-KD-247 antibodies in monkey plasma (1 : 400 dilution) were measured using samples collected at necropsy. Binding activity indicated that the number of anti-KD-247 antibodies in Cy-6 was significantly higher than in the other monkeys (Fig. 2a). To clarify the sites of recognition of the anti-KD-247 antibodies in Cy-6, the binding activity of antibodies in Cy-6 plasma to other anti-HIV-1 antibodies was investigated. Rμ5.5 is a reshaped mAb that is equivalent to the entire KD-247 molecule except for antigen-binding sites [6,20], and Cβ1 is a chimeric mAb whose Fc region is equivalent to that of KD-247 [21]. These mAbs were used, as well as KD-247 coated for ELISA. The reaction of these mAbs with the monkey antibodies was detected by biotinylated KD-247 based on a double-antibody capture ELISA. The antibodies bound to KD-247 in Cy-6 plasma reacted with neither Rμ5.5 nor Cβ1 (Fig. 2b). Finally, we examined whether anti-KD-247 antibodies in Cy-6 plasma inhibit the binding of KD-247 to antigen peptides. Two KD-247-specific antigen peptides, SP13 and P20PATH (NNTRRRLSIGPGRA-FYARRN), derived from the V3 region of SHIV-C2/1, were coated on ELISA plates and reacted with KD-247 that had been incubated overnight at 4°C with Cy-6 plasma collected on day 0, day 7, or at necropsy. Binding of KD-247 to antigen peptides decreased by approximately 60% after reaction of mAb with Cy-6 plasma collected at necropsy (Fig. 2c). Antibody inhibition of the binding of KD-247 to antigen peptides strongly suggests that the plasma contained an antiidiotype antibody.

Suppression of plasma viral load and of $CD4^+$ T-cell loss in peripheral blood

The kinetics of plasma viral load in monkey plasma is shown in Fig. 3(a). The viral loads were suppressed in monkeys given KD-247 in comparison with those given control IgG. The complete protection previously reported with preadministration of KD-247 was not achieved in these postadministration trials [7]. The $CD4^+$ T-cell counts were maintained at higher levels in monkeys given KD-247 than in the control animals (Fig. 3b). The suppression of viral load and the maintenance effect of KD-247 on $CD4^+$ T cells were similar among the test groups. As each group had only two animals, between-group significant differences were not tested.

Maintenance of $CD4^+$ T cells in various lymphoid tissues

At 11–13 weeks after viral challenge, necropsies of the monkeys given KD-247 were performed and their lymphoid organs were evaluated. All the lymph nodes of the monkeys inoculated with pathogenic SHIV followed by control IgG were atrophied. In contrast, the lymph nodes of all monkeys given KD-247 maintained normal shape. Marked change was observed in the thymus (Fig. 4a); the thymuses of all monkeys given KD-247 were hypertrophic, whereas the thymuses of monkeys inoculated with SHIV alone, or given control IgG, were atrophied. No organ atrophy was observed in any of the

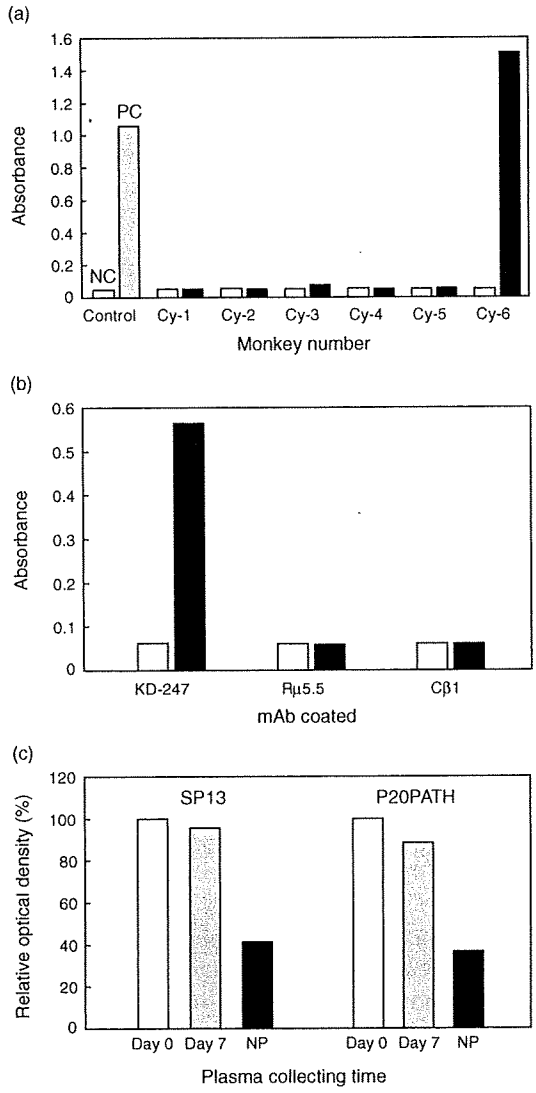

Fig. 2. Properties of anti-KD-247 antibodies in Cy-6 monkey plasma. (a) Anti-KD-247 activity of plasma in monkeys given KD-247. Open and closed bars indicate the binding activities of anti-KD-247 antibodies to KD-247 in monkey plasma collected at day 0 and necropsy, respectively. NC, negative control using the sample diluent; PC, positive control using a goat antibody to human IgG (200 ng/ml; ICN/Cappel, Aurora, Ohio, USA). (b) Binding of Cy-6 plasma to humanized and chimeric mAbs. Open and closed bars indicate binding activities of anti-KD-247 antibodies to KD-247 in monkey plasma collected on day 0 and at necropsy (day 88), respectively. (c) Inhibitory effect of Cy-6 plasma on the binding of KD-247 to antigen peptides SP13 (left) and P20PATH (right). The plasma samples collected on day 7 and at necropsy had been incubated with these peptides. Suppression of the binding of KD-247 to the peptides is shown as relative optical density (%) to the binding of KD-247 incubated with plasma collected on day 0. IgG, immunoglobulin G; NP, necropsy.

groups treated with KD-247. To determine the architecture of the lymph nodes, we examined tissue sections collected at necropsy. Germinal centers were not detected in the lymphoid tissue of monkeys treated with control IgG, but cell architecture was preserved in monkeys given KD-247 (Fig. 4b).

The T-cell subpopulation in the lymphoid tissues of the monkeys was analyzed by flow cytometry (Fig. 5). The $CD4^+$ T cells in the lymph nodes of both the IgG control monkeys (Cy-7 and Cy-8) were nearly depleted. In contrast, a normal level of $CD4^+CD8^-$ cells was maintained in the lymph nodes of all monkeys given KD-247. The $CD4^+CD8^-$ T-cell population values in the groups given KD-247 and control IgG were obviously higher and lower, respectively, than the values for the mean − 2 SD in naive control monkeys ($n = 15$). In the thymus, the absolute cell numbers of the monkeys given control IgG were low and could not be assessed for Cy-7 lymphocytes because of cell depletion. Thymic T-cell subpopulations were composed almost entirely of $CD4^+CD8^+$ double-positive cells (Cy-1 = 52%, Cy-2 = 74%, Cy-3 = 75%, Cy-4 = 76%, Cy-5 = 77%, Cy-6 = 75%, and Cy-8 = 71%; naive = 63 ± 15%). In the submandibular and mesenteric lymph nodes and spleen, administration of KD-247 rescued $CD4^+CD8^-$ cells independently of injection timing; this T-cell subset was not maintained in IgG controls.

Discussion

Since the development of HAART, the likelihood of progression to AIDS or death has been decreased if $CD4^+$ T-cell counts are properly maintained even when HIV-1 RNA concentrations in peripheral blood are high [22]. This finding suggests importance of maintaining $CD4^+$ T cells in the whole body for the control of HIV/AIDS. In this study, we confirmed that postinfection passive immunization of SHIV-infected monkeys with KD-247 fully rescued $CD4^+$ T-cell loss in various lymphoid tissues and yielded partial protection against increased plasma viral load and loss of $CD4^+$ T cells.

How, then, does postinfection immunization with KD-247 help maintain $CD4^+$ T cells in lymphoid tissues? Immunohistological alterations of the lymph nodes in HIV-infected patients represent a dynamic process, in which an initial florid follicular hyperplasia gives way ultimately to lymphocyte depletion [23]. There are several theories regarding the various direct or indirect mechanisms of $CD4^+$ lymphocyte depletion by HIV [24]. We previously reported that treatment with the humanized neutralizing antibody Rμ5.5 prevented HIV-1-induced atrophic changes in the medulla of engrafted thymic tissue in a thymus/liver-transplanted severe combined immunodeficient murine model [20]. The acute pathogenic SHIV-C2/1-derived clone virus KS661 resulted in increased thymic involution, atrophy, and the depletion of immature T cells, including $CD4^+CD8^+$ double-positive cells [25]. Infection with HIV-1, SIV, or

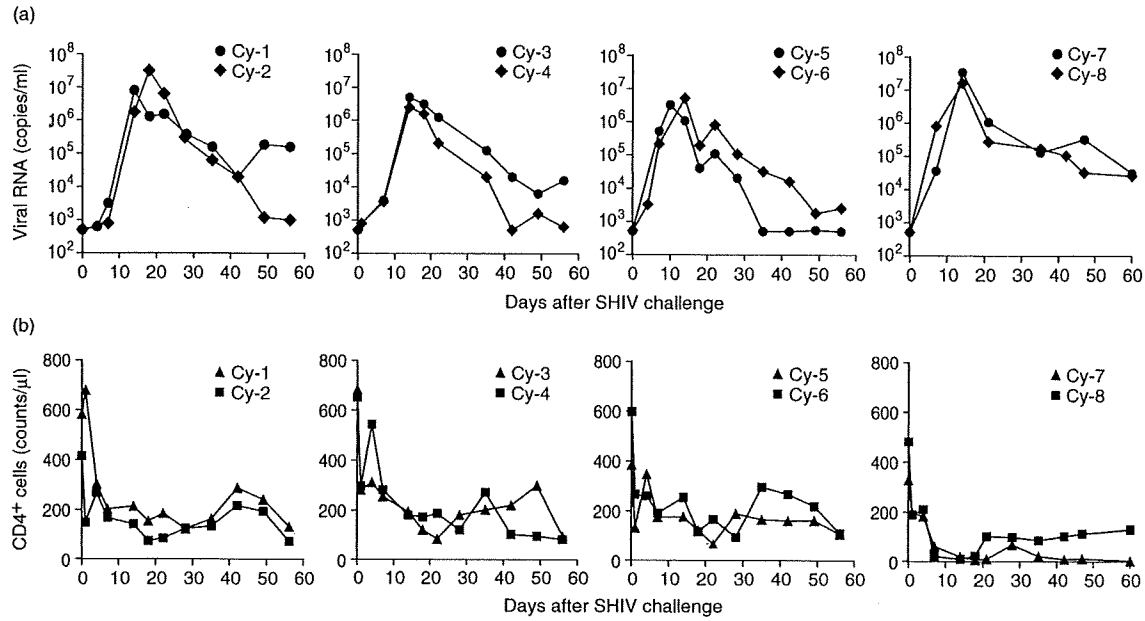

Fig. 3. Plasma viral loads and CD4$^+$ T-cell counts after viral challenge. Postchallenge plasma viral RNA copies and absolute CD4$^+$ T-cell counts in the peripheral blood were detected in the monkeys in each of four groups treated with KD-247 antibody or control IgG after infection as described in Fig. 1(a). (a) Kinetic changes in viral RNA copy numbers per ml of peripheral blood. (b) Kinetics of CD4$^+$ T-cell counts. IgG, immunoglobulin G; SHIV, simian/human immunodeficiency virus.

SHIV is associated with abnormalities in the number, size, and structure of germinal centers [26]. Progressive depletion of proliferating B cells and disruption of the follicular dendritic cell network in germinal centers within 20 days after SIV challenge have also been reported [27]. Although our study was limited by small group size (two monkeys/group), our data clearly show only minimal differences in CD4$^+$ T-cell levels between groups treated with KD-247 and the IgG control monkeys. The effects of KD-247 on CD4$^+$ T cells were more remarkable in lymph node than in peripheral blood compartments. Accumulation of apoptotic cells has been reported in both lymph nodes and thymus during the second week of highly pathogenic SHIV-C2/1 [17,28] and $SHIV_{DH12R}$ infections [29]. Given the smaller increase in CD4$^+$CD95$^+$ cell populations in peripheral blood mononuclear cells among monkeys that exhibited even partial protection from postchallenge SHIV-C2/1 with a suboptimal dose of KD-247 infusion in previous studies [7], KD-247 might protect against apoptosis of CD4$^+$ T cells in lymphoid tissues. Thus, in addition to neutralizing antibodies in animals receiving transfusions, passive transfer of KD-247 might help to maintain levels of CD4$^+$ T cells and to preserve the integrity of lymphoid structures, potentially leading to a less pathogenic course of disease progression. The roles played by the antibodies against HIV/AIDS could be clarified by further analyses of immunological function of monkeys treated with KD-247; areas of future research include viral components [30,31], lymphocyte activation [32,33], cytokine spectra [34], T-cell homeostasis [35,36], dendritic cell functions [37,38], Fc receptor interactions [39,40], and related functions.

Because preinfection experiments have shown that the concentration of KD-247 in plasma is important in protecting monkeys against viral infection [7], we also measured KD-247 concentrations in plasma samples. The postinfection effect of KD-247 against increased viral load and CD4$^+$ T-cell loss in peripheral blood were evaluated. Monkeys given KD-247 had lower plasma viral loads and less CD4$^+$ T-cell loss than did those treated with control IgG; however, as noted above, each group had only two animals and no statistical analysis was performed. These results in peripheral blood were not very pronounced compared with the phenomena observed in lymphoid organs. Complete protection, which was previously reported with preinfection administration of KD-247 [7], was not achieved in these postinfection trials. The times and values of viral load peaks were similar in all monkeys, but the increases in viral loads were delayed by administration of KD-247. Interestingly, the ability of KD-247 to suppress viral loads after they peaked did not depend on the timing of administration. In previous preinfection experiments with 45 mg/kg of KD-247, viral challenges were performed 1 day after KD-247 administration, and blood concentrations of KD-247 ranged from 700 to 800 μg/ml immediately before viral challenge in monkeys. Preadministration of these concentrations of KD-247 yielded complete protection against SHIV-C2/1 infection [7]. By contrast, in the current study, the monkeys given KD-247 1 h after

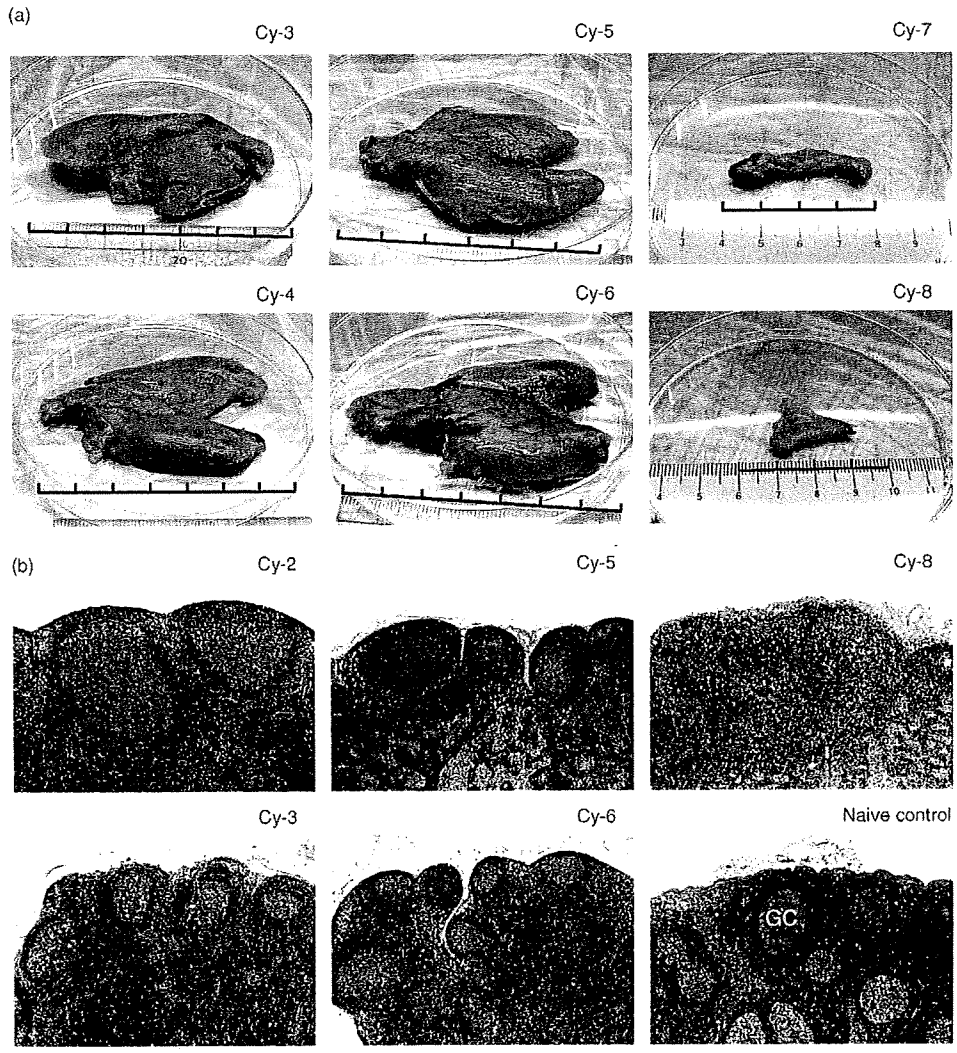

Fig. 4. Comparative postinfection protection against atrophic changes in lymphoid tissues. (a) Macroscopic images of thymus. Superimposed rulers indicate scales marked in centimeters. Although Cy-1, Cy-2, and naive control thymuses are not shown here, all thymuses of the monkeys given KD-247 were larger and those given control IgG were smaller than naive monkey thymuses. (b) Histological changes as postinfection effects of KD-247. Parts of the tissue blocks were preserved in 10% buffered formalin, embedded in paraffin. Tissue sections were stained with hematoxylin and eosin for conventional light microscopy (original magnification 18×). Mesenteric (Cy-2, Cy-5, and Cy-6), inguinal (Cy-3 and naive control), and submandibular (Cy-8) lymph nodes were photographed. Germinal centers, which are bright round areas (shown as GC in only the naive control), were maintained in the monkeys given KD-247, whereas the architecture of germinal centers in lymph node tissue from the control monkey given human normal IgG was not detected. GC, germinal centers; IgG, immunoglobulin G.

challenge with the virus became infected, even though the KD-247 concentrations 15 min after administration ranged from 1000 to 1300 μg/ml (Fig. 1b i). These KD-247 concentrations are considered sufficient to neutralize cell-free viruses that develop after the initial infection and/or are generated one after another following infection in peripheral blood. Therefore, the inability of the antibody administered 1 h after challenge to completely protect against the virus suggests that target cells were infected with the virus within 1 h. The previously reported results of time-dependence studies [10,11,41] of postinfection prophylaxis using SHIV are comparable with those obtained in the present study. The virus might not only infect target cells directly but also evade neutralizing antibody to produce infection in the cells of the peripheral blood and/or the lymphoid tissues [42,43]. Follicular dendritic cells could sustain HIV infection in the presence of neutralizing antibody [44]. Mucosal infection, such as vaginal challenge with SHIV, has been suggested to be a better in-vivo model to evaluate passive immunization [45,46]. The effects of antibodies in the lymph node compartment might be clearly observable using models of mucosal infection, as viruses harbored in lymph nodes after mucosal challenge later appeared in the peripheral blood compartment following systemic spread. Unexpectedly,

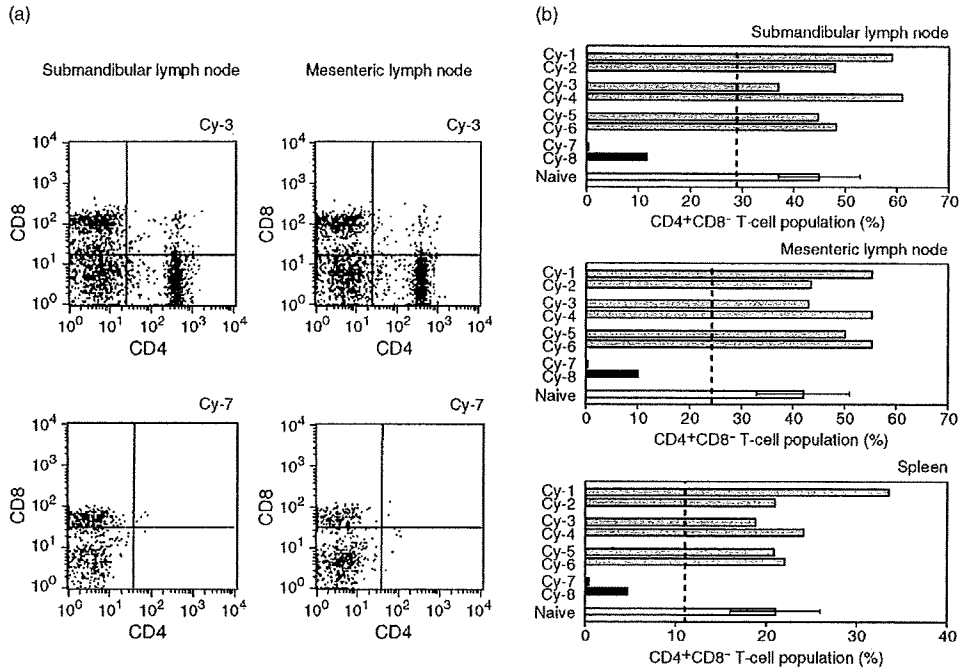

Fig. 5. Postinfection protection against tissue CD4$^+$ T-cell loss by passive transfer of KD-247 at various times after simian/human immunodeficiency virus C2/1 challenge. (a) Flow cytometric profiles of CD4$^+$ and CD8$^+$ T cells in the submandibular (left) and mesenteric (right) lymph nodes. Upper panels show maintenance of CD4$^+$ T cells in animal Cy-3 after passive transfer of KD-247. Lower panels show the loss of CD4$^+$ populations in the control IgG-treated animal Cy-7. (b) Postinfection protection of KD-247 against loss of CD4$^+$CD8$^-$ tissue lymphocytes. Tissue distributions of CD4$^+$CD8$^-$ T cells were determined in submandibular and mesenteric lymph nodes and spleen in animals of each group, as well as in those of naive control monkeys ($n = 15$). Bars indicate SD. Broken lines show the mean – 2 SD values of the naive control. IgG, immunoglobulin G.

the maintenance of CD4$^+$ T cells in the lymph nodes in Cy-6 were similar to those in the other monkeys given KD-247, although the mAb was eliminated from the plasma 3 weeks after viral challenge, once anti-KD-247 antibodies were elicited in this monkey. High plasma concentrations of KD-247 seem to be effective in preventing HIV-1 transmission. However, even if high concentrations are not maintained in the blood for a long time, KD-247 could rescue lymphoid CD4$^+$ T cells.

Passive immunization with mAbs has been shown to prevent a variety of diseases, although no mAb products are licensed for use for immunotherapy against HIV/AIDS [47]. In a passive immunization trial with humans, a cocktail of three mAbs was able to delay viral rebound following interruption of antiretroviral therapy [15]. However, differences in the pharmacokinetic profiles of constituent mAbs and cost-related issues of production might affect the development of neutralizing mAb cocktail drugs [47,48]. In contrast, KD-247 itself neutralizes primary isolates including chemokine (C–C motif) receptor 5 (CCR5)-tropic viruses with a matching narrow-neutralization sequence motif [6,7]. KD-247 is expected to be useful as a novel reagent for immune protection against HIV/AIDS, because the mAb might not only directly neutralize the virus but also maintain CD4$^+$ T cells in lymphoid tissues.

Acknowledgements

This work was supported by the 'Panel on AIDS' of the United States–Japan Cooperative Medical Science Program and the Health Science Foundation, Japan.

T. Murakami planned experiments, wrote the manuscript, and analyzed the laboratory data; M. Honda conducted the study, planned the experiments, and wrote the manuscript; Y. Eda planned and conducted the experiments; T. Nakasone, K. Someya, N. Yoshino, M. Kaizu, and Y. Izumi performed the animal experiments and analyzed the laboratory data; Y. Ami and H. Matsui performed the animal experiments and the pathological analyses; K. Shinohara managed the animal experiments; N. Yamamoto supervised the study.

Part of the information was presented at the 16th Annual Meeting of the Japanese Society for AIDS Research, 28–30 November 2002, Nagoya, Japan (abstract 249).

References

1. Douek DC, Kwong PD, Nabel GJ. **The rational design of an AIDS vaccine.** *Cell* 2006; **124**:677–681.
2. McMichael AJ. **HIV vaccines.** *Annu Rev Immunol* 2006; **24**: 227–255.

3. Haynes BF, Montefiori DC. **Aiming to induce broadly reactive neutralizing antibody responses with HIV-1 vaccine candidates.** *Expert Rev Vaccines* 2006; **5**:579–595.
4. Lin G, Nara PL. **Designing immunogens to elicit broadly neutralizing antibodies to the HIV-1 envelope glycoprotein.** *Curr HIV Res* 2007; **5**:514–541.
5. Emini EA, Schleif WA, Nunberg JH, Conley AJ, Eda Y, Tokiyoshi S, *et al.* **Prevention of HIV-1 infection in chimpanzees by gp120 V3 domain-specific monoclonal antibody.** *Nature* 1992; **355**:728–730.
6. Eda Y, Takizawa M, Murakami T, Maeda H, Kimachi K, Yonemura H, *et al.* **Sequential immunization with V3 peptides from primary human immunodeficiency virus type 1 produces cross-neutralizing antibodies against primary isolates with a matching narrow-neutralization sequence motif.** *J Virol* 2006; **80**: 5552–5562.
7. Eda Y, Murakami T, Ami Y, Nakasone T, Takizawa M, Someya K, *et al.* **Anti-V3 humanized antibody KD-247 effectively suppresses ex vivo generation of human immunodeficiency virus type 1 and affords sterile protection of monkeys against a heterologous simian/human immunodeficiency virus infection.** *J Virol* 2006; **80**:5563–5570.
8. Matsushita S, Takahama S, Shibata J, Kimura T, Shiosaki K, Eda Y, *et al.* **Ex vivo neutralization of HIV-1 quasi-species by a broadly reactive humanized monoclonal antibody KD-247.** *Hum Antibodies* 2005; **14**:81–88.
9. Haigwood NL, Montefiori DC, Sutton WF, McClure J, Watson AJ, Voss G, *et al.* **Passive immunotherapy in simian immunodeficiency virus-infected macaques accelerates the development of neutralizing antibodies.** *J Virol* 2004; **78**:5983–5995.
10. Nishimura Y, Igarashi T, Haigwood NL, Sadjadpour R, Donau OK, Buckler C, *et al.* **Transfer of neutralizing IgG to macaques 6 h but not 24 h after SHIV infection confers sterilizing protection: implications for HIV-1 vaccine development.** *Proc Natl Acad Sci U S A* 2003; **100**:15131–15136.
11. Ferrantelli F, Buckley KA, Rasmussen RA, Chalmers A, Wang T, Li P-L, *et al.* **Time dependence of protective postexposure prophylaxis with human monoclonal antibodies against pathogenic SHIV challenge in newborn macaques.** *Virology* 2007; **358**:69–78.
12. Ruprecht RM, Ferrantelli F, Kitabwalla M, Xu W, McClure HM. **Antibody protection: passive immunization of neonates against oral AIDS virus challenge.** *Vaccine* 2003; **21**:3370–3373.
13. Safrit JT, Ruprecht R, Ferrantelli F, Xu W, Kitabwalla M, Van Rompay K, *et al.*, Ghent IAS Working Group on HIV in Women and Children. **Immunoprophylaxis to prevent mother-to-child transmission of HIV-1.** *J Acquir Immune Defic Syndr* 2004; **35**:169–177.
14. Hammer SM, Saag MS, Schechter M, Montaner JSG, Schooley RT, Jacobsen DM, *et al.*, International AIDS Society-USA panel. **Treatment for adult HIV infection: 2006 recommendations of the International AIDS Society-USA panel.** *JAMA* 2006; **296**: 827–843.
15. Trkola A, Kuster H, Rusert P, Joos B, Fischer M, Leemann C, *et al.* **Delay of HIV-1 rebound after cessation of antiretroviral therapy through passive transfer of human neutralizing antibodies.** *Nat Med* 2005; **11**:615–622.
16. Shinohara K, Sakai K, Ando S, Ami Y, Yoshino N, Takahashi E, *et al.* **A highly pathogenic simian/human immunodeficiency virus with genetic changes in cynomolgus monkey.** *J Gen Virol* 1999; **80**:1231–1240.
17. Sasaki Y, Ami Y, Nakasone T, Shinohara K, Takahashi E, Ando S, *et al.* **Induction of CD95 ligand expression on T lymphocytes and B lymphocytes and its contribution to apoptosis of CD95-up-regulated CD4+ T lymphocytes in macaques by infection with a pathogenic simian/human immunodeficiency virus.** *Clin Exp Immunol* 2000; **122**:381–389.
18. Kaizu M, Sato H, Ami Y, Izumi Y, Nakasone T, Tomita Y, *et al.* **Infection of macaques with an R5-tropic SHIV bearing a chimeric envelope carrying subtype E V3 loop among subtype B framework.** *Arch Virol* 2003; **148**:973–988.
19. Yoshino N, Ami Y, Terao K, Tashiro F, Honda M. **Upgrading of flow cytometric analysis for absolute counts, cytokines and other antigenic molecules of cynomolgus monkeys (*Macaca fascicularis*) by using antihuman cross-reactive antibodies.** *Exp Anim* 2000; **49**:97–110.
20. Okamoto Y, Eda Y, Ogura A, Shibata S, Amagai T, Katsura Y, *et al.* **In SCID-hu mice, passive transfer of a humanized antibody prevents infection and atrophic change of medulla in human thymic implant due to intravenous inoculation of primary HIV-1 isolate.** *J Immunol* 1998; **160**:69–76.
21. Matsushita S, Maeda H, Kimachi K, Eda Y, Maeda Y, Murakami T, *et al.* **Characterization of a mouse/human chimeric monoclonal antibody (Cβ1) to a principal neutralizing domain of the human immunodeficiency virus type 1 envelope protein.** *AIDS Res Hum Retroviruses* 1992; **8**:1107–1115.
22. Egger M, May M, Chêne G, Phillips AN, Ledergerber B, Dabis F, *et al.*, and the ART Cohort Collaboration. **Prognosis of HIV-1-infected patients starting highly active antiretroviral therapy: a collaborative analysis of prospective studies.** *Lancet* 2002; **360**:119–129.
23. Wood GS. **The immunohistology of lymph nodes in HIV infection: a review.** *Prog AIDS Pathol* 1990; **2**:25–32.
24. Cloyd MW, Chen JJY, Adeqboyega P, Wang L. **How does HIV cause depletion of CD4 lymphocytes? A mechanism involving virus signaling through its cellular receptors.** *Curr Mol Med* 2001; **1**:545–550.
25. Motohara M, Ibuki K, Miyake A, Fukazawa Y, Inaba K, Suzuki H, *et al.* **Impaired T-cell differentiation in the thymus at the early stages of acute pathogenic chimeric simian-human immunodeficiency virus (SHIV) infection in contrast to less pathogenic SHIV infection.** *Microbes Infect* 2006; **8**:1539–1549.
26. Margolin DH, Saunders EH, Bronfin B, de Rosa N, Axthelm MK, Goloubeva OG, *et al.* **Germinal center function in the spleen during simian HIV infection in rhesus monkeys.** *J Immunol* 2006; **177**:1108–1119.
27. Zhang Z-Q, Casimiro DR, Schleif WA, Chen M, Citron M, Davies M-E, *et al.* **Early depletion of proliferating B cells of germinal center in rapidly progressive simian immunodeficiency virus infection.** *Virology* 2007; **361**:455–464.
28. Yoshino N, Ryu T, Sugamata M, Ihara T, Ami Y, Shinohara K, *et al.* **Direct detection of apoptotic cells in peripheral blood from highly pathogenic SHIV-inoculated monkey.** *Biochem Biophys Res Commun* 2000; **268**:868–874.
29. Igarashi T, Brown CR, Byrum RA, Nishimura Y, Endo Y, Plishka RJ, *et al.* **Rapid and irreversible CD4+ T-cell depletion induced by the highly pathogenic simian/human immunodeficiency virus $SHIV_{DH12R}$ is systemic and synchronous.** *J Virol* 2002; **76**:379–391.
30. Gratton S, Cheynier R, Dumaurier M-J, Oksenhendler E, Wain-Hobson S. **Highly restricted spread of HIV-1 and multiply infected cells within splenic germinal centers.** *Proc Natl Acad Sci U S A* 2000; **97**:14566–14571.
31. de Paiva GR, Laurent C, Godel A, da Silva NA Jr, March M, Delsol G, *et al.* **Discovery of human immunodeficiency virus infection by immunohistochemistry on lymph node biopsies from patients with unexplained follicular hyperplasia.** *Am J Surg Pathol* 2007; **31**:1534–1538.
32. Zamarchi R, Barelli A, Borri A, Petralia G, Ometto L, Masiero S, *et al.* **B cell activation in peripheral blood and lymph nodes during HIV infection.** *AIDS* 2002; **16**:1217–1226.
33. Biancotto A, Iglehart SJ, Vanpouille C, Condack CE, Lisco A, Ruecker E, *et al.* **HIV-1-induced activation of CD4+ T cells creates new targets for HIV-1 infection in human lymphoid tissue ex vivo.** *Blood* 2008; **111**:699–704.
34. Biancotto A, Grivel J-C, Iglehart SJ, Vanpouille C, Lisco A, Sieg SF, *et al.* **Abnormal activation and cytokine spectra in lymph nodes of people chronically infected with HIV-1.** *Blood* 2007; **109**:4272–4279.
35. Nokta MA, Li X-D, Nichols J, Pou A, Asmuth D, Pollard RB. **Homeostasis of naive and memory T cell subpopulations in peripheral blood and lymphoid tissues in the context of human immunodeficiency virus infection.** *J Infect Dis* 2001; **183**:1336–1342.
36. Letvin NL, Mascola JR, Sun Y, Gorgone DA, Buzby AP, Xu L, *et al.* **Preserved CD4+ central memory T cells and survival in vaccinated SIV-challenged monkeys.** *Science* 2006; **312**:1530–1533.
37. Taruishi M, Terashima K, Dewan Z, Dewan MZ, Yamamoto N, Ikeda S, *et al.* **Role of follicular dendritic cells in the early HIV-1 infection: in vitro model without specific antibody.** *Microbiol Immunol* 2004; **48**:693–702.

38. Turville SG, Aravantinou M, Stössel H, Romani N, Robbiani M. **Resolution of de novo HIV production and trafficking in immature dendritic cells.** *Nat Methods* 2008; **5**:75–85.
39. Forthal DN, Landucci G, Phan TB, Becerra J. **Interactions between natural killer cells and antibody Fc result in enhanced antibody neutralization of human immunodeficiency virus type 1.** *J Virol* 2005; **79**:2042–2049.
40. Wilflingseder D, Banki Z, Garcia E, Pruenster M, Pfister G, Muellauer B, *et al.* **IgG opsonization of HIV impedes provirus formation in and infection of dendritic cells and subsequent long-term transfer to T cells.** *J Immunol* 2007; **178**:7840–7848.
41. Foresman L, Jia F, Li Z, Wang C, Stephans EB, Sahni M, *et al.* **Neutralizing antibodies administered before, but not after, virulent SHIV prevent infection in macaques.** *AIDS Res Hum Retroviruses* 1998; **14**:1035–1043.
42. Chen JJ-Y, Huang JC, Shirtliff M, Briscoe E, Ali S, Cesani F, *et al.* **CD4 lymphocytes in the blood of HIV$^+$ individuals migrate rapidly to lymph nodes and bone marrow: support for homing theory of CD4 cell depletion.** *J Leukoc Biol* 2002; **72**:271–278.
43. Malaspina A, Moir S, Nickle DC, Donoghue ET, Ogwaro KM, Ehler LA, *et al.* **Human immunodeficiency virus type 1 bound to B cells: relationship to virus replicating in CD4$^+$ T cells and circulating in plasma.** *J Virol* 2002; **76**:8855–8863.
44. Heath SL, Tew JG, Tew JG, Szakal AK, Burton GF. **Follicular dendritic cells and human immunodeficiency virus infectivity.** *Nature* 1995; **377**:740–744.
45. Kahn JO, Walker BD. **Acute human immunodeficiency virus type 1 infection.** *N Engl J Med* 1998; **339**:33–39.
46. Mascola JR. **Passive transfer studies to elucidate the role of antibody-mediated protection against HIV-1.** *Vaccine* 2002; **20**:1922–1925.
47. Bansal GP. **A summary of the workshop on passive immunization using monoclonal antibodies for HIV/AIDS, held at the National Institute of Allergy and Infectious Diseases, Bethesda, 10 March 2006.** *Biologicals* 2007; **35**:367–371.
48. Joos B, Trkola A, Kuster H, Aceto L, Fischer M, Stiegler G, *et al.* **Long-term multiple-dose pharmacokinetics of human monoclonal antibodies (mAbs) against human immunodeficiency virus type 1 envelope gp120 (mAb 2G12) and gp41 (mAbs 4E10 and 2F5).** *Antimicrob Agents Chemother* 2006; **50**:1773–1779.

ANTIMICROBIAL AGENTS AND CHEMOTHERAPY, July 2009, p. 2940–2948 Vol. 53, No. 7
0066-4804/09/$08.00+0 doi:10.1128/AAC.01727-08

The Novel CXCR4 Antagonist KRH-3955 Is an Orally Bioavailable and Extremely Potent Inhibitor of Human Immunodeficiency Virus Type 1 Infection: Comparative Studies with AMD3100▽

Tsutomu Murakami,[1]† Sei Kumakura,[2]† Toru Yamazaki,[2] Reiko Tanaka,[3] Makiko Hamatake,[1] Kazu Okuma,[3]‡ Wei Huang,[4] Jonathan Toma,[4] Jun Komano,[1] Mikiro Yanaka,[2]§ Yuetsu Tanaka,[3] and Naoki Yamamoto[1]*

AIDS Research Center, National Institute of Infectious Diseases, Tokyo 162-8640,[1] Biomedical Research Laboratories, Kureha Corporation, Tokyo 169-8503,[2] and Department of Immunology, Graduate School and Faculty of Medicine, University of the Ryukyus, Nakagami, Okinawa 903-0215,[3] Japan, and Monogram Biosciences, South San Francisco, California 94080[4]

Received 30 December 2008/Returned for modification 12 February 2009/Accepted 7 May 2009

The previously reported CXCR4 antagonist KRH-1636 was a potent and selective inhibitor of CXCR4-using (X4) human immunodeficiency virus type 1 (HIV-1) but could not be further developed as an anti-HIV-1 agent because of its poor oral bioavailability. Newly developed KRH-3955 is a KRH-1636 derivative that is bioavailable when administered orally with much more potent anti-HIV-1 activity than AMD3100 and KRH-1636. The compound very potently inhibits the replication of X4 HIV-1, including clinical isolates in activated peripheral blood mononuclear cells from different donors. It is also active against recombinant X4 HIV-1 containing resistance mutations in reverse transcriptase and protease and envelope with enfuvirtide resistance mutations. KRH-3955 inhibits both SDF-1α binding to CXCR4 and Ca^{2+} signaling through the receptor. KRH-3955 inhibits the binding of anti-CXCR4 monoclonal antibodies that recognize the first, second, or third extracellular loop of CXCR4. The compound shows an oral bioavailability of 25.6% in rats, and its oral administration blocks X4 HIV-1 replication in the human peripheral blood lymphocyte-severe combined immunodeficiency mouse system. Thus, KRH-3955 is a new promising agent for HIV-1 infection and AIDS.

The chemokine receptors CXCR4 and CCR5 serve as major coreceptors of human immunodeficiency virus type 1 (HIV-1), along with CD4 as a primary receptor for virus entry (2, 15, 18, 19). SDF-1α, which is a ligand for CXCR4, blocks the infection of CXCR4-utilizing X4 HIV-1 strains (7, 34). On the other hand, ligands for CCR5 such as RANTES inhibit CCR5-utilizing R5 HIV-1 (10). These findings made chemokines, chemokine derivatives, or small-molecule inhibitors of chemokine receptors attractive candidates as a new class of anti-HIV-1 agents. Many CCR5 antagonists have been developed as anti-HIV-1 drugs. These include TAK-779 (Takeda Pharmaceutical Company) (5), TAK-652 (6), TAK-220 (45), SCH-C (Schering-Plough) (43), SCH-D (vicriviroc) (42), GW873140 (aplaviroc; Ono Pharmaceutical/Glaxo Smith Kline) (28), and UK-427,857 (maraviroc; Pfizer Inc.) (17). Of these, maraviroc was approved by the U.S. FDA in 2007 for the treatment of R5 HIV-1 in treatment-experienced adult patients, combined with other antiretroviral treatment. Several classes of CXCR4 antagonists have also been reported. The bicyclam AMD3100 showed antivirus activity against many X4 and some R5X4 HIV strains in peripheral blood mononuclear cells (PBMCs) but not against R5 strains (16, 40). The pharmacokinetics and antiviral activity of this compound were also evaluated in humans (21, 22). T22, [Tyr-5,12, Lys-7]polyphemusin II, which is an 18-mer peptide derived from horseshoe crab blood cells, was reported to specifically inhibit X4 HIV-1 strains (30). Studies on the pharmacophore of T140 (a derivative of T22) led to the identification of cyclic pentapeptides (46).

In 2003, we reported that KRH-1636 is a potent and selective CXCR4 antagonist and inhibitor of X4 HIV-1 (23). Although the compound was absorbed efficiently from the rat duodenum, it has poor oral bioavailability. Continuous efforts to find more potent CXCR4 antagonists that are bioavailable when administered orally allowed us to develop KRH-3955 by a combination of chemical modification of the lead compound and biological assays. In this report, we describe the results of a preclinical evaluation of KRH-3955, including its in vitro anti-HIV-1 activity, its in vivo efficacy in the human peripheral blood lymphocyte (hu-PBL)-severe combined immunodeficiency (SCID) mouse model, and its pharmacokinetics in rats in comparison with those of AMD3100.

* Corresponding author. Mailing address: AIDS Research Center, National Institute of Infectious Diseases, 1-23-1 Toyama, Shinjuku-ku, Tokyo 162-8640, Japan. Phone: 81-3-5285-1111, ext. 2302. Fax: 81-3-5285-1165. E-mail: nyama@nih.go.jp.

† T.M. and S.K. contributed equally to this work.

‡ Present address: Department of Safety Research on Blood and Biological Products, National Institute of Infectious Diseases, Gakuen 4-7-1, Musashimurayama-shi, Tokyo 208-0011, Japan.

§ Present address: Kureha Special Laboratory Co., Ltd., Fukushima 974-8232, Japan.

▽ Published ahead of print on 18 May 2009.

MATERIALS AND METHODS

Compounds. The synthesis and purification of KRH-3955, *N,N*-dipropyl-*N'*-{4-({[(1*H*-imidazol-2-yl)methyl][(1-methyl-1*H*-imidazol-2-yl)methyl]amino}methyl)benzyl]-*N'*-methylbutane-1,4-diamine tri-(2*R*,3*R*)-tartrate, were carried out by Kureha Corporation. The chemical structure of KRH-3955 is shown in Fig. 1. The CXCR4 antagonist AMD3100 and zidovudine (AZT) were obtained from Sigma. Saquinavir was obtained

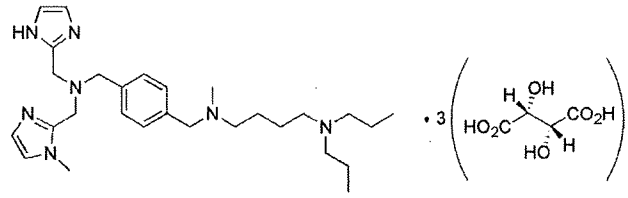

FIG. 1. Chemical structure of KRH-3955.

from the NIH AIDS Research and Reference Reagent Program, NIAID, Bethesda, MD. AMD070 and SCH-D were synthesized at Kureha Corporation.

Cells. Molt-4 no. 8 cells (24) were maintained in RPMI 1640 medium (Invitrogen, Carlsbad, CA) supplemented with 10% fetal bovine serum (Sigma, St. Louis, MO) and antibiotics (50 ng/ml penicillin, 50 ng/ml streptomycin, and 100 ng/ml neomycin; Invitrogen), which is referred to as RPMI medium. Chemokine receptor-expressing human embryonic kidney 293 (HEK293) cells (ATCC CRL-1573) and Chinese hamster ovary (CHO) cells (ATCC CCL-61) were maintained in minimal essential medium or F-12 (Invitrogen) supplemented with 10% fetal bovine serum and antibiotics (50 ng/ml penicillin, 50 ng/ml streptomycin, and 100 ng/ml neomycin). PBMCs from HIV-1-seronegative healthy donors were isolated by Ficoll-Hypaque density gradient (Lymphosepal; IBL, Gunma, Japan) centrifugation (31) and grown in RPMI medium supplemented with recombinant human interleukin-2 (rhIL-2; Roche, Mannheim, Germany) at 50 U/ml.

Viruses. Viral stocks of HIV-1_{NL4-3}, HIV-1_{JR-CSF}, and HIV-$1_{89.6}$ were each produced in the 293T cell line by transfection with HIV-1 molecular clone plasmids pNL4-3 (1), pYK-JRCSF (25), and p89.6 (11), respectively, by the calcium phosphate method. The 50% tissue culture infective dose was determined by an end-point assay with PBMC cultures activated with immobilized anti-CD3 monoclonal antibody (MAb) (33, 51). Subtype B HIV-1 primary isolates 92HT593, 92HT599 (N. Hasley), and 91US005 (B. Hahn) and AZT-resistant HIV-1 (A018) (D. D. Richman) (26) were obtained from the AIDS Research and Reference Reagent Program, Division of AIDS, NIAID, NIH. These clinical isolates were propagated in the activated PBMCs prepared as described above.

Anti-HIV-1 assays. Human PBMCs activated with immobilized anti-CD3 MAb (OKT-3; ATCC, Manassas, VA) in RPMI medium for 3 days were infected with various HIV-1 strains, including primary clinical isolates, at a multiplicity of infection of 0.001. After 3 h of adsorption, the cells were washed and cultured in RPMI medium supplemented with rhIL-2 (50 U/ml) in the presence or absence of the test compounds. Amounts of HIV-1 capsid (p24) antigen produced in the culture supernatants were measured by an enzyme-linked immunosorbent assay kit (ZeptoMetrix Corp., Buffalo, NY) 7 to 10 days after infection. The cytotoxicities of the compounds were tested on the basis of the viability and proliferation of the activated PBMCs, as determined with Cell Proliferation Kit II (XTT) from Roche (36).

Susceptibility of multidrug-resistant HIV-1 to CXCR4 antagonists was also measured by using recombinant viruses in a single replication cycle assay (9, 49). HIV-1 resistance test vectors (RTVs) contain the entire protease (PR) coding region and the reverse transcriptase (RT) coding region, from amino acid 1 to amino acid 305, amplified from patient plasma and a luciferase expression cassette inserted in the *env* region. The RTVs in this study contain patient-derived PR and RT sequences that possess mutations associated with resistance to PR, RT, or both PR and RT. Env-pseudotyped viruses were produced by cotransfecting 293 cells with RTV plasmids and expression vectors encoding the Env protein of well-characterized X4-tropic laboratory strain HXB2, NL4-3, or NL4-3 containing the Q40H enfuvirtide (T20) resistance mutation introduced by site-direct mutagenesis. The virus stocks were harvested 2 days after transfection and used to infect U87 $CD4^+$ cells (kind gifted from N. Landau, NYU School of Medicine) expressing CXCR4 in 96-well plates, with serial dilutions of CXCR4 antagonists. Target cells were lysed, and luciferase activity was measured to assess virus replication in the presence and absence of inhibitors. Drug concentrations required to inhibit virus replication by 50% (IC_{50}) were calculated.

Immunofluorescence. Molt-4 cells or CXCR4-expressing HEK293 cells were treated with various concentrations of KRH-3955 or AMD3100 in RPMI medium or phosphate-buffered saline containing 1% bovine serum albumin and 0.05% NaN_3 (fluorescence-activated cell sorting [FACS] buffer). In washing experiments, cells were washed with RPMI medium or FACS buffer. The cells were Fc blocked with 2 mg/ml normal human immunoglobulin G (IgG) in FACS buffer and then stained directly with mouse MAbs 12G5-phycoerythrin (PE) and 44717-PE (R&D Systems, Inc., Minneapolis, MN) or rat MAb A145-fluorescein isothiocyanate (FITC) and indirectly with MAb A80. The A145 and A80 MAbs were produced in ascitic fluid of BALB/c nude mice, and IgG fractions were obtained from ascitic fluid by gel filtration chromatography with Superdex G200 (Amersham Pharmacia). Goat anti-rat IgG (heavy and light chains) labeled with FITC was purchased from American Corlex (47). After washing, the cells were analyzed on a FACScalibur (BD Biosciences, San Jose, CA) flow cytometer with CellQuest software (BD Biosciences).

DNA construction and transfection. Chemokine receptor-expressing CHO cells were generated as reported previously (23). Human CXCR4 cDNA was cloned into the pcDNA3.1 vector. Mutations were introduced by using the QuikChange II site-directed mutagenesis kit (Stratagene, La Jolla, CA). All constructs were verified by DNA sequencing and transfected into 293 cells by using the Lipofectamine reagent (Invitrogen) (48). Stable transfectants were selected in the presence of 400 μg/ml G418 (Invitrogen). The COOH-terminal intracellular domain of CXCR4 (residues 308 to 352) was deleted in all mutants and the wild type. This deletion has no influence on HIV-1 infection or on SDF-1α binding and signaling but abolishes ligand-induced endocytosis (3).

Ligand-binding assays. Chemokine receptor-expressing CHO cells (5×10^6/0.2 ml per well) were cultured in a 24-well microtiter plate. After 24 h of incubation at 37°C, the culture medium was replaced with binding buffer (RPMI medium supplemented with 0.1% bovine serum albumin). Binding reactions were performed on ice in the presence of ^{125}I-labeled chemokines (final concentration of 100 pmol/liter; PeproTech Inc., Rocky Hill, NJ) and various concentrations of test compounds. After washing away of unbound ligand, cell-associated radioactivity was counted with a scintillation counter as described previously (23).

CXCR4-mediated Ca^{2+} signaling. Fura2-acetoxymethyl ester (Dojindo Laboratories, Kumamoto, Japan)-loaded CXCR4-expressing CHO cells were incubated in the absence or presence of various concentrations of KRH-3955 or AMD3100. Changes in intracellular Ca^{2+} levels in response to SDF-1α (1 μg/ml) were determined by using a fluorescence spectrophotometer as described previously (30).

Detection of KRH-3955 in blood after oral administration. The plasma concentration-time profile of R-176211 (distilled water was used as a vehicle), the free form of KRH-3955, was examined after a single oral administration of KRH-3955 at a dose of 10 mg/kg or intravenous administration at a dose of 10 mg/kg to male Sprague-Dawley rats (CLEA, Kanagawa, Japan). R-176211 in plasma was measured by liquid chromatography-tandem mass spectrometry. Pharmacokinetic parameters were calculated by using WinNonlin Professional (ver. 3.1; Pharsight Co.).

Infection of hu-PBL–SCID mice. Two groups of C.B-17 SCID mice (CLEA, Kanagawa, Japan) were administered a single dose of either KRH-3955 or tartrate (2% glucose solution was used as the vehicle) as a control orally (p.o.) and fed for 2 weeks. These mice were then engrafted with human PBMCs (1×10^7 cells/animal intraperitoneally [i.p.]) and after 1 day were infected i.p. with 1,000 infective units of X4 HIV-1_{NL4-3}. IL-4 (2 μg per animal) was administrated i.p. on days 0 and 1 after PBMC engraftment to enhance X4 HIV-1 infection. After 7 days, human lymphocytes were collected from the peritoneal cavities and spleens of the infected mice and cultured in vitro for 4 days in RPMI medium supplemented with 20 U/ml rhIL-2. HIV-1 infection was monitored by measuring p24 levels in the culture supernatant. We used a selected donor whose PBMCs could be engrafted at an efficiency of >80% in C.B-17 SCID mice. Usually, 5×10^5 to 10×10^5 human $CD4^+$ T cells can be recovered from each hu-PBL–SCID mouse. Mice with no or low recovery of human $CD4^+$ T cells at the time of analysis were omitted. For ex vivo cultures, we used a quarter of the cells recovered from a mouse. The protocols for the care and use of the hu-PBL–SCID mice were approved by the Committee on Animal Research of the University of the Ryukyus before initiation of the present study.

RESULTS

Anti-HIV-1 activities of KRH-3955 in activated PBMCs. The inhibitory activity of KRH-3955 against X4 HIV-1 (NL4-3), R5X4 HIV-1 (89.6), and R5 HIV-1 (JR-CSF) was examined in activated human PBMCs from two different donors. KRH-3955 inhibited the replication of both X4 and R5X4 HIV-1 in activated PBMCs with 50% effective concentrations (EC_{50}) of 0.3 to 1.0 nM but did not affect R5 HIV-1 replication, even at concentration of up to 200 nM (Table 1). In contrast, the CCR5 antagonist SCH-D (vicriviroc) inhibited R5 HIV-1 rep-

TABLE 1. Anti-HIV-1 activity of KRH-3955 in activated PBMCs[a]

Virus	Donor	EC_{50} (nM)[b]					
		KRH-3955	AMD3100	AMD070	SCH-D	AZT	SQV
NL4-3	A	1.1	41	35	>1,000	11	9.0
X4	B	0.33	15	15	>1,000	8.0	29
89.6	A	0.38	44	55	>1,000	7.4	9.9
R5X4	B	ND[c]	ND	ND	ND	ND	ND
JR-CSF	A	>200	>200	>200	0.37	0.96	2.6
R5	B	>200	>200	>200	1.2	6.2	8.0
A018H (X4) (pre-AZT)	C	1.4	38	ND	ND	1.9	ND
A018G (X4) (post-AZT)	C	1.3	32	ND	ND	87.000	ND

[a] PBMCs from two different donors were used in each assay. Anti-HIV-1 activity was determined by measuring the p24 antigen level in culture supernatants.
[b] Assays were carried out in triplicate wells. The average of two to four experiments is shown.
[c] ND, not determined.

lication but inhibited neither X4 nor R5X4 HIV-1 replication (Table 1). The anti-HIV activity of KRH-3955 against the 89.6 virus from donor B was not determined because the virus did not replicate enough for calculation of the anti-HIV activity of KRH-3955 and other drugs. Notably, the anti-HIV-1 activity of KRH-3955 was much higher than that of AMD3100, a well-known X4 HIV-1 inhibitor, or AMD070, the other X4 inhibitor that is bioavailable when administered orally. KRH-3955 also inhibited the replication of clinical isolates of X4 HIV-1 (92HT599) and R5X4 HIV-1 (92HT593) with EC_{50} ranging from 4.0 to 4.2 nM (data not shown). Although both KRH-3955 and AMD3100 were effective against at least some R5X4 HIV-1 strains in activated PBMCs, neither KRH-3955 nor AMD3100 inhibited the infection of CD4/CCR5 cells by R5 or R5X4 HIV-1, even at a concentration of 1,660 nM (data not shown). Importantly, the 50% cytotoxic concentration of KRH-3955 in activated PBMCs (donor A) was 57 μM, giving a high therapeutic index (51,818) in the case of NL4-3 infection, which was higher than that of AZT (8,000 in the case of donor A). These results indicate that the compound is a selective inhibitor of HIV-1 that can utilize CXCR4 as a coreceptor. Since a CXCR4 antagonist should be used in combination with a CCR5 antagonist in a clinical setting, we next examined whether the combined use of both antagonists efficiently blocks mixed infection with X4 and R5 HIV-1. Combination of KRH-3955 and SCH-D at 4 plus 4 nM and 20 plus 20 nM blocked the replication of 50:50 mixtures of NL4-3 and JR-CSF by 91 and 96%, respectively (data not shown). Thus, KRH-3955 is a highly potent and selective inhibitor of X4 HIV-1.

Anti-HIV-1 activities of KRH-3955 in activated PBMCs from different donors. It has been observed that the anti-HIV-1 activity of compounds in PBMCs varies from donor to donor. Therefore, the anti-HIV-1 activity of KRH-3955 against X4 HIV-1 was examined in activated PBMCs from eight different donors. The levels of p24 antigen in NL4-3-infected cultures ranged from 17 to 120 ng/ml (Table 2). KRH-3955 inhibited the replication of NL4-3 with EC_{50} ranging from 0.23 to 1.3 nM and with EC_{90} ranging from 2.7 to 3.5 nM (Table 2), demonstrating that the anti-HIV-1 activity of KRH-3955 was independent of the PBMC donor.

Anti-HIV-1 activities of KRH-3955 against drug-resistant HIV-1 strains. To further assess the efficacy of KRH-3955, we used a single-cycle assay to evaluate the activity of KRH-3955 against a panel of recombinant viruses that express an X4-tropic envelope protein (HXB2) but contain PR and RT sequences containing a wide variety of mutations associated with resistance to PR inhibitors (PIs), nucleoside RT inhibitors (NRTIs), and non-NRTIs (NNRTIs). This assessment was also performed with recombinant viruses that express an X4-tropic envelope protein (NL4-3) that contains the Q40H mutation and displays resistance to T20 (an entry inhibitor). The results of these experiments demonstrate that both KRH-3955 and AMD3100 inhibited the infection of CD4/CXCR4 cells by these recombinant drug-resistant viruses, including viruses resistant to PIs, NRTIs, or NNRTIs; multidrug-resistant viruses; and T20-resistant viruses (Table 3). We also observed that KRH-3955 inhibited the replication of A018G, a highly AZT-resistant strain, in activated PBMCs with an EC_{50} of 1.3 nM (Table 1).

KRH-3955 selectively inhibits ligand binding to CXCR4. To investigate whether KRH-3955 specifically blocks ligand binding to CXCR4, the inhibitory effect of the compound on chemokine binding to CHO cells expressing CXCR4, CXCR1, CCR2b, CCR3, CCR4, or CCR5 was determined. KRH-3955 efficiently inhibited SDF-1α binding to CXCR4 in a dose-dependent manner (Fig. 2 and 3b), and the IC_{50} for SDF-1α binding was 0.61 nM, which is similar to its EC_{50} against HIV-1. Similar results were obtained when we used a Molt-4 T cell line as the CXCR4-expressing target cell (Fig. 3a). Interestingly, the inhibitory activity of AMD3100 against SDF-1α binding was much weaker than its anti-HIV-1 activity (Fig. 3), suggesting that the binding sites of these two compounds are different. In contrast, the compound did not affect the binding

TABLE 2. Anti-HIV-1 activity of KRH-3955 against NL4-3 infection of PBMCs from eight different donors

Donor	p24 level (ng/ml)	EC_{50} (nM)	EC_{90} (nM)
1	31	1.30	3.2
2	25	1.20	3.2
3	17	1.20	3.3
4	40	0.70	2.9
5	120	0.77	2.9
6	58	1.50	3.5
7	49	0.23	2.7
8	53	1.00	3.0
Mean ± SD	49 ± 32	0.99 ± 0.40	3.1 ± 0.30

TABLE 3. KRH-3955 susceptibilities of drug-resistant viruses[a]

Virus[b]	IC_{50} (nM)[c]	
	KRH-3955	AMD3100
NL4-3	0.50	4.6
HXB2	0.60	6.2
NRTI-Res (HXB2-env)	0.60	9.0
NNRTI-Res (HXB2-env)	0.80	7.0
PI-Res (HXB2-env)	0.70	9.2
MDR (HXB2-env)	0.70	5.3
T20-Res (NL4-3-env)	0.40	2.3

[a] Susceptibility of drug-resistant HIV-1 was measured by using a single-cycle recombinant virus assay (see Materials and Methods).
[b] The pseudoviruses containing X4-tropic envelope (HXB2 or NL4-3) and patient-derived PR and RT sequences containing mutations associated with resistance to PR (PI-Res), RT (NRTI-Res or NNRTI-Res), or both (MDR) (the mutations are not shown). T20-Res contains a site-directed mutation (Q40H) in the NL4-3 envelope.
[c] IC50, 50% inhibitory concentration of CXCR4 antagonists.

of ^{125}I-labeled SDF-1α, ^{125}I-labeled RANTES, ^{125}I-labeled MCP-1, ^{125}I-labeled TARC, ^{125}I-labeled RANTES, or ^{125}I-labeled IL-8 to CXCR4, CCR1, CCR2b, CCR4, CCR5, or CXCR1, respectively (Fig. 2). Thus, KRH-3955 selectively blocks the binding of SDF-1α to CXCR4.

KRH-3955 exhibits inhibition of Ca^{2+} signaling through CXCR4. We next examined whether KRH-3955 acts as an agonist or antagonist of CXCR4 by using CXCR4-expressing CHO cells. The addition of KRH-3955 inhibited the SDF-1α-induced increase in the intracellular Ca^{2+} concentration in a dose-dependent manner, whereas 100 nM AMD3100 did not affect Ca^{2+} mobilization (Fig. 4). KRH-3955 itself did not affect Ca^{2+} mobilization at up to 1 μM (data not shown). We performed the Ca^{2+} mobilization assay with human PBMCs but could not detect an SDF-1α-induced Ca^{2+} signal mainly due to low expression of CXCR4 (data not shown). Thus, KRH-3955 inhibits Ca^{2+} signaling through CXCR4.

Effect of KRH-3955 on anti-CXCR4 antibody binding to CXCR4-expressing cells. To localize the binding site(s) of KRH-3955, the effects of KRH-3955 and AMD3100 on the binding of four types of anti-CXCR4 MAbs were first examined. We used MAbs A145, 12G5, 44717, and A80, which are specific for the N terminus, extracellular loop 1 (ECL1) and ECL2, ECL2, and ECL3, respectively. Neither KRH-3955 nor AMD3100 inhibited A145 binding to CXCR4-expressing Molt-4 cells (Fig. 5). Both compounds inhibited the binding of MAbs 12G5, 44717, and A80 to Molt-4 cells in a dose-depen-

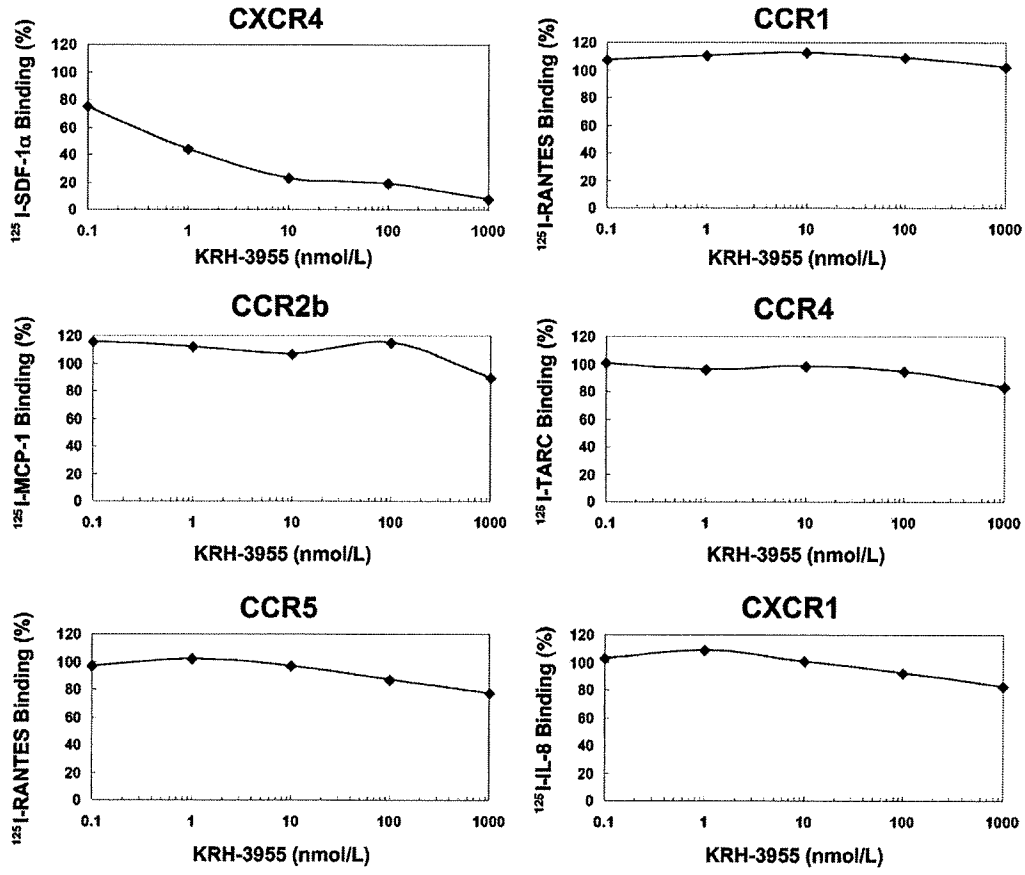

FIG. 2. Inhibitory effects of KRH-3955 on chemokine binding to CXCR4-, CCR1-, CCR2b-, CCR4-, CCR5-, or CXCR1-expressing CHO cells. Chemokine receptor-expressing CHO cells were incubated with various concentrations of KRH-3955 in binding buffer containing ^{125}I-labeled chemokine. Binding reactions were performed on ice and were terminated by washing out the unbound ligand. Cell-associated radioactivity was measured with a scintillation counter. Percent binding was calculated as 100 × [(binding with inhibitor − nonspecific binding)/(binding without inhibitor − nonspecific binding)]. The data represent the means in duplicate wells in a single experiment.

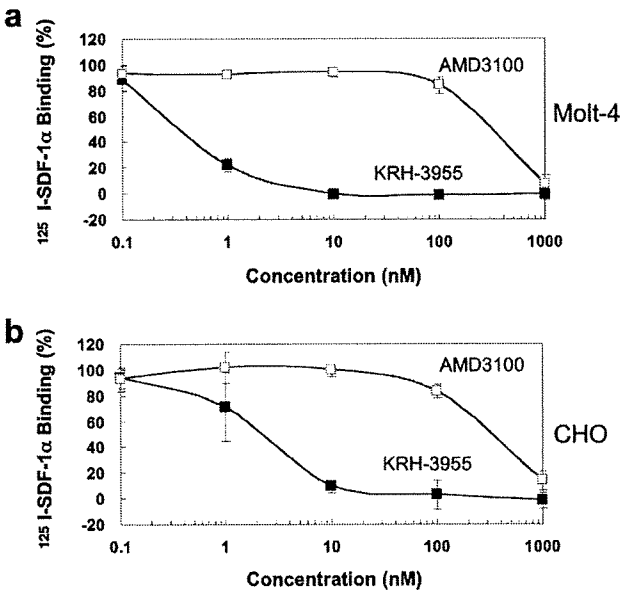

FIG. 3. Concentration-dependent inhibition by KRH-3955 of SDF-1α binding to (a) Molt-4 and (b) CXCR4-expressing CHO cells. CXCR4-expressing CHO cells were incubated with various concentrations of KRH-3955 (■) or AMD3100 (□) in binding buffer containing ^{125}I-labeled SDF-1α. Binding reactions were performed, and percent binding was calculated as described in the legend to Fig. 2. The data represent the means ± standard deviations of three independent experiments.

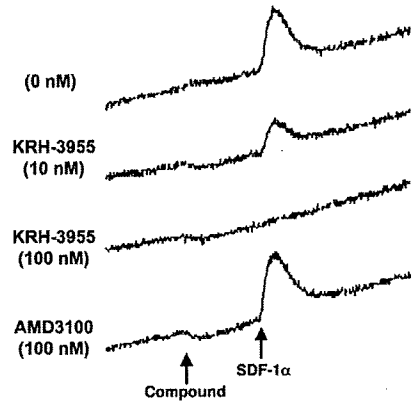

FIG. 4. Inhibitory effects of KRH-3955 on SDF-1α-induced Ca^{2+} mobilization in CXCR4-expressing CHO cells. Fura-2-acetoxymethyl ester-loaded CXCR4-expressing CHO cells were incubated in the presence or absence of various concentrations of KRH-3955 or AMD3100. Changes in intracellular Ca^{2+} levels in response to SDF-1α (1 μg/ml) were determined with a fluorescence spectrophotometer. The data show representative data for two independent experiments.

dent manner. The inhibitory activity of KRH-3955 is similar to its anti-HIV-1 activity, whereas the inhibitory activity of AMD3100 is much weaker than its anti-HIV-1 activity. Similar data were obtained when activated human PBMCs were used as target cells (data not shown). KRH-3955 itself did not induce internalization of CXCR4 at concentrations of up to 1 μM (data not shown), as KRH-1636 did (23). These results suggest that the binding sites of KRH-3955 are located in a region composed of all three ECLs of CXCR4.

Long-lasting inhibitory effects of KRH-3955 on the binding of MAb 12G5. The inhibitory effect of KRH-3955 on the binding of MAb 12G5 was examined with or without washing of the compound from the cells. Molt-4 cells were treated with 10 nM KRH-3955 or 1,000 nM AMD3100 for 15 min. With or without washing, the cells were stained with MAb 12G5-PE and the amount of bound antibody was analyzed by flow cytometry. KRH-3955 strongly inhibited MAb 12G5 binding to Molt-4 cells irrespectively of washing (Fig. 6a). In contrast, AMD3100 efficiently inhibited MAb 12G5 binding without washing away of the compound but lost its inhibitory activity after washing away of the compound (Fig. 6a). The long-lasting inhibitory effect of KRH-3955 on the binding of MAb 12G5 was further tested. Molt-4 cells were preincubated with or without KRH-3955 at 10 nM. The compound was washed away, and the cells were further incubated at 37°C in compound-free growth medium. At 0, 3, and 6 h after compound removal, the cells were stained with MAb 12G5-PE and analyzed by flow cytometry. Even at 6 h after washing away of the compound, KRH-3955 inhibited MAb 12G5 binding by approximately 40% (Fig. 6b). These results suggest that KRH-3955 has a strong binding affinity for CXCR4 and a slow dissociation rate, although competition assays with the two molecules (KRH-3955 versus MAb 12G5 with radioactive, nonradioactive, or different labeling) are necessary to provide definitive conclusions.

Inhibition of MAb 12G5 binding to CXCR4 mutants by KRH-3955. The effects of different CXCR4 mutations on the inhibitory activity of KRH-3955 against MAb 12G5 binding to CXCR4 were examined. HEK293-CXCR4 transfectants were preincubated with various concentrations of KRH-3955 and AMD3100, after which the compound was washed away. The binding of PE-conjugated MAb 12G5 was measured by flow cytometry. As reported previously, AMD3100 substantially lost its blocking activity against MAb 12G5 binding for D171A (TM4), D262A (TM6), and E288A/L290A (TM7) mutants, as shown by previous reports (Table 4) (20, 37, 38). In contrast, the blocking activity of KRH-3955 against MAb 12G5 binding was not affected by the above mutations. In contrast, the H281A (ECL3) mutant displayed decreased inhibition of MAb 12G5 binding by KRH-3955 (Table 4). These data further support the hypothesis that the CXCR4 interaction sites of KRH-3955 are different from those of AMD3100.

Pharmacokinetic studies of KRH-3955 in rats. In pharmacokinetics studies, KRH-3955 was orally or intravenously administrated to Sprague-Dawley rats at a dose of 10 mg/kg. The plasma concentration of R-176211, the free form of KRH-3955, was monitored by liquid chromatography-tandem mass spectrometry. In these studies, KRH-3955 was found to be well absorbed and the absolute oral bioavailability in rats was calculated to be 25.6% based on the area under the plasma concentration-time curve (Table 5). However, KRH-3955 also showed a long elimination half-life after single-dose administration to rats, suggesting long-term accumulation of the compound in tissues (Table 5). KRH-3955 was found to be stable in human hepatic microsomes, and no significant inhibition of CYP450 liver enzymes by this compound was observed (data

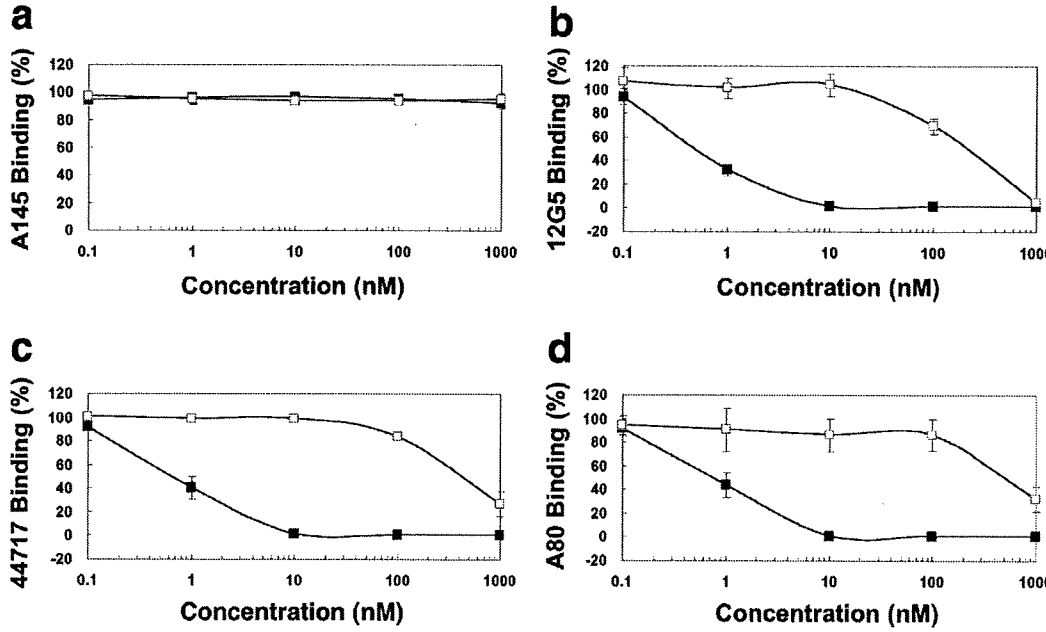

FIG. 5. Effect of KRH-3955 on the binding of four different MAbs to the CXCR4 receptor. Molt-4 cells were incubated with various concentrations of KRH-3955 (■) or AMD3100 (□). The cells were stained directly with MAbs 12G5 (recognizes ECL1 and ECL2 of CXCR4)-PE, 44717 (recognizes ECL2 of CXCR4)-PE, and A145 (recognizes the N terminus of CXCR4)-FITC or indirectly with MAb A80 (recognizes ECL3 of CXCR4). The mean fluorescence of the stained cells was analyzed with a FACScalibur flow cytometer. Percent binding was calculated with the equation described in the legend to Fig. 2. The data represent the means ± standard deviations of three independent experiments.

not shown). Thus, orally administered KRH-3955 is bioavailable in rats.

KRH-3955 efficiently suppresses X4 HIV-1 infection in hu-PBL–SCID mice. We then examined whether KRH-3955 can interfere with X4 HIV-1 infection in vivo by using hu-PBL–SCID mice. Mice were administrated a single dose (10 mg/kg) of either KRH-3955 or tartrate (as a control) p.o. and fed for 2 weeks. These mice were then engrafted with human PBMCs, and after 1 day, these "humanized" mice were infected with infectious X4 HIV-1 (NL4-3). After 7 days, human lymphocytes harvested from the peritoneal cavities and spleens of the infected mice were cultured for 4 days in vitro in the presence of rhIL-2 in order to determine the level of HIV-1 infection by the p24 enzyme-linked immunosorbent assay. The maximum concentration of KRH-3955 in blood after p.o. administration was estimated to be 100 nM (data now shown). Under these conditions, four of five mock-treated mice were infected whereas only one of five mice treated with KRH-3955 was infected (Table 6). The one infected mouse in the KRH-3955-treated group (no. 5)

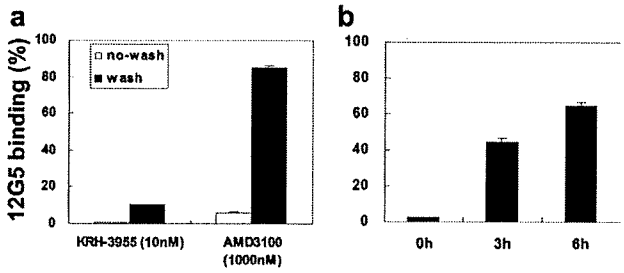

FIG. 6. Long-lasting inhibitory effects of KRH-3955 on the binding of MAb 12G5. (a) Molt-4 cells were treated with 10 nM KRH-3955 or 1,000 nM AMD3100 for 15 min. With (■) or without (□) washing, the cells were staining with MAb 12G5-PE and analyzed by flow cytometry. (b) Long-lasting inhibitory effect of KRH-3955 on the binding of MAb 12G5. Molt-4 cells were preincubated with or without KRH-3955 at 10 nM. The compound was washed away, and the cells were further incubated at 37°C in compound-free RPMI medium. At 0, 3, and 6 h after removal of the compound, the cells were staining with MAb 12G5-PE and analyzed by flow cytometry. The data represent the means of triplicate wells in a single experiment.

TABLE 4. Affinity of KRH-3955 and AMD3100 for wild-type CXCR4 and various mutant forms of CXCR4[a]

CXCR4 (location)	KRH-3955		AMD3100	
	IC_{50}	IC_{90}	IC_{50}	IC_{90}
Wild type	2.8 ± 0.5	8.2 ± 0.4	289.1 ± 25.5	971.1 ± 31.2
V99A (ECL1)	1.5 ± 0.2	7.4 ± 0.2	258.5 ± 25.9	>1,000
V112A (TM3)	2.2 ± 0.2	>10	196.6 ± 28.5	821.3 ± 15.4
H113A (TM3)	0.8 ± 0.3	6.3 ± 0.2	296.4 ± 112.2	>1,000
D171A (TM4)	3.2 ± 0.1	>10	>1,000	>1,000
D181A (ECL2)	0.5 ± 0.1	5.1 ± 0.3	143.7 ± 29.3	795.6 ± 79.9
H203A (TM5)	0.5 ± 0.1	5.3 ± 0.1	259.0 ± 11.5	860.6 ± 22.4
D262A (TM6)	1.6 ± 0.3	8.1 ± 0.5	>1,000	>1,000
E275A (ECL3)	1.0 ± 0.2	6.4 ± 0.1	235.6 ± 30.2	930.2 ± 26.1
E277A (ECL3)	3.1 ± 0.1	8.7 ± 0.1	469.5 ± 19.2	>1,000
V280A (ECL3)	1.0 ± 0.2	6.1 ± 0.1	175.3 ± 10.3	821.2 ± 47.3
H281A (ECL3)	14.1 ± 5.2	248.3 ± 74.9	72.7 ± 42.9	572.2 ± 118.1
W283A (ECL3)	1.3 ± 0.2	6.9 ± 0.2	300.2 ± 10.5	>1,000
I284A (TM7)	1.2 ± 0.2	6.8 ± 0.5	265.8 ± 20.8	>1,000
E288A/L290A (TM7)	1.6 ± 0.1	7.7 ± 0.3	>1,000	>1,000

[a] The data shown, which represent means ± SDs (n = 3) of nanomolar concentrations, were obtained from competition binding on HEK293 cells expressing the wild-type or mutant CXCR4 receptors with MAb 12G5.

TABLE 5. Pharmacokinetic parameters of KRH-3955 after single oral administration in rats[a]

Parameter	Value when given i.v. or p.o. at 10 mg/kg
Bioavailability (%)[b]	25.6
I.v. half-life (h)	99.0 ± 13.1
I.v. CL (liters/h/kg)[c]	3.9 ± 0.07
V_1 (ss) (liters/kg)[d]	374.0 ± 14
P.o. C_{max} (ng/ml)[e]	86.3 ± 23.6
T_{max} (h)[f]	2.3 ± 1.53
P.o. $AUC_{0\text{-}336}$ (ng · h/ml)[g]	325.0 ± 38

[a] The data shown are means ± SDs (n = 3).
[b] Bioavailability = $(AUC_{oral}/AUC_{i.v.}) \times (dose_{i.v.}/dose_{oral}) \times 100$.
[c] CL, clearance.
[d] V_1 (ss), volume of distribution in central compartment at steady state.
[e] C_{max}, maximum concentration of drug in serum.
[f] T_{max}, time to maximum concentration of drug in serum.
[g] $AUC_{0\text{-}336}$, area under the plasma concentration-time curve from time zero to 336 h.

TABLE 6. Inhibition of infection of hu-PBL–SCID mice with X4 HIV-1 by KRH-3955[a]

Group and mouse no.	p24 produced (pg/ml)
Control	
1	747
2	10,263
3	<5
4	5,821
5	1,902
KRH-3955	
6	<5
7	<5
8	<5
9	<5
10	36

[a] Two groups of C.B-17 SCID mice (n = 5) were administrated a single dose of either KRH-3955 or tartrate (as a control) p.o. and fed for 2 weeks. These mice were then engrafted with human PBMCs (1×10^7 per animal i.p.), and after 1 day, these "humanized" mice were infected with 1,000 infective units of X4 $HIV\text{-}1_{NL4\text{-}3}$. IL-4 (2 mg per animal) was administrated i.p. on days 0 and 1 after PBMC engraftment to enhance X4 HIV-1 infection. After 7 days, human lymphocytes were harvested from the infected mice and cultured in vitro for 4 days in medium containing 20 U/ml IL-2. HIV-1 infection was monitored by measuring p24 levels. Means from duplicate determinations are shown. <5, below detection level.

showed low levels of p24 production. These results indicate that single-dose p.o. administration of KRH-3955 was very effective in protecting against X4 HIV-1 infection in an in vivo mouse model.

DISCUSSION

In this study, we clearly demonstrate that KRH-3955, a KRH-1636 derivative that is bioavailable when administered orally, is a potent inhibitor of HIV-1 infection both in vitro and in vivo. KRH-3955 selectively inhibited X4 HIV-1 strains, including clinical isolates, as we have previously shown with KRH-1636. Furthermore, KRH-3955 is approximately 40 times more potent than KRH-1636 in its anti-HIV-1 activity in activated PBMCs (Table 1). The anti-HIV-1 activity of KRH-3955 was independent of the PBMC donor (Table 2). KRH-3955 also inhibited the infectivity of recombinant viruses resistant to NRTIs, NNRTIs, PIs, and T20 (Table 3). Pharmacokinetic studies of KRH-3955 indicated that the compound is bioavailable in rats when administered orally (Table 5). In addition, oral administration of the compound efficiently inhibited the replication of X4 HIV-1 in the hu-PBL–SCID mouse model (Table 6). Although we could show that KRH-3955 is a potent inhibitor of subtype B HIV-1 isolates, we need to examine the efficacy of this compound against non-subtype B HIV-1 isolates because of the global nature of the HIV/AIDS epidemic and the regional diversity of HIV-1 subtypes.

R5 HIV-1 is isolated predominantly during the acute and asymptomatic stage (12) and is also believed to be important for virus transmission between individuals. In contrast, X4 HIV-1 strains emerge in approximately 50% of infected individuals and their emergence is associated with a rapid $CD4^+$ T-cell decline and disease progression (35, 50). One recent report also indicated that detection of X4 HIV-1 at baseline independently predicted disease progression (13), although it is still not known whether the emergence of X4 HIV-1 is a cause or outcome of disease progression. These findings strongly support the need for highly potent CXCR4 inhibitors that are bioavailable when administered orally such as KRH-3955.

Inhibition of ligand binding to chemokine receptors by KRH-3955 was specific for CXCR4 (Fig. 2), as we observed previously for KRH-1636. This specific inhibition of SDF-1α binding to CXCR4 by KRH-3955 is absolutely necessary for developing an anti-HIV agent to avoid immune dysregulation by nonspecific inhibition of binding by other chemokines. It is of note that the inhibitory activity of the compound against SDF-1α binding is similar to that against HIV-1 infection, which is different from that of control compound AMD3100. Where on the CXCR4 molecule is the binding site(s) of KRH-3955? Experiments to examine the effect of KRH-3955 on the binding of several anti-CXCR4 MAbs suggest that the binding sites of KRH-3955 are located in all three ECLs of CXCR4 (Fig. 5). To further define the binding site(s) of KRH-3955, we examined the effects of CXCR4 point mutations on the inhibitory activity of KRH-3955 against MAb 12G5 binding to the receptor. AMD3100 was used as a control. The inhibitory activity of AMD3100 against MAb 12G5 binding to the receptor was greatly reduced by the mutations D171A (TM4), D262A (TM6), and E288A/L290A (TM7), as reported previously (Table 4) (20, 37, 38). Of note, these mutations also affect SDF-1α binding and/or CXCR4 coreceptor activity (8). Unexpectedly, none of these three mutations affected the inhibition of MAb 12G5 binding by KRH-3955 (Table 4). Only the H281A (ECL3) mutant showed decreased inhibition of MAb 12G5 binding by KRH-3955 (Table 4). Interestingly, the same mutant modestly increased the blocking activity of AMD3100 against MAb 12G5 binding. In addition, the H281A mutation markedly impaired inhibition of MAb 12G5 binding by AMD3465, one of the prototype monocyclams (37). Further experiments with different CXCR4 mutants are necessary to identify the exact site(s) on CXCR4 targeted by this compound.

Pharmacological tests of KRH-3955 were performed with rats, and the compound was found to be bioavailable when administered orally (Table 5), which is favorable for anti-HIV drugs. However, the compound also indicated a long half-life after single-dose administration to rats, suggesting long-term accumulation of the compound in tissues, which can be either advantageous

in terms of inhibiting HIV-1 infection in hu-PBL–SCID mice (Table 6) or disadvantageous in terms of toxicity. Further studies are ongoing to determine the safety and pharmacokinetics of the compound in other animals such as dogs and monkeys. To evaluate the in vivo efficacy of KRH-3955, we used the hu-PBL–SCID mouse model and showed that oral administration of the compound strongly protected against X4 HIV-1 infection in this model system (Table 6). To achieve substantial replication of X4 HIV-1 in this system, recombinant IL-4 was added after human PBMC engraftment as described previously (23). Notably, KRH-3955 was administered only once 2 weeks before PBMC engraftment and was effective enough to block X4 HIV-1 infection, suggesting that the compound can be used as a preexposure prophylaxis agent to prevent HIV infection. This long-lasting antiviral effect of KRH-3955 can be partly explained by the strong affinity of the compound for CXCR4 (Fig. 6) and long-term accumulation of the compound in tissues.

In terms of safety of anti-HIV drugs, CCR5 antagonists are considered to be relatively safe because of the lack of obvious health problems in individuals homozygous for the CCR5 delta32 allele (27, 39). Indeed, maraviroc, a CCR5 antagonist, was approved by the U.S. FDA in 2007. In contrast, CXCR4 antagonists, which inhibit SDF-1α–CXCR4 interactions, may cause severe adverse effects because knocking out either the SDF-1α or the CXCR4 gene in mice causes marked defects such as abnormal hematopoiesis and cardiogenesis, in addition to vascularization of the gastrointestinal tract (32, 44, 52). However, no severe side effects have been reported for either AMD3100, a well-characterized CXCR4 antagonist, or AMD070, an oral CXCR4 antagonist, in human volunteers and/or HIV-infected patients. Milder side effects, including gastrointestinal symptoms and paresthesias, were common at higher doses of AMD3100. These results indicate the feasibility of using CXCR4 antagonists as anti-HIV-1 drugs in a clinical setting (21, 22, 41).

Besides the physiological roles mentioned above, the CXCR4–SDF-1 axis is also involved in various diseases such as cancer metastasis, leukemia cell progression, rheumatoid arthritis, and pulmonary fibrosis. CXCR4 antagonists such as AMD3100 and T140 have demonstrated activity in treating such CXCR4-mediated diseases (14, 46). In addition, AMD3100 is considered to be a stem cell mobilizer for transplantation in patients with cancers such as non-Hodgkin's lymphoma. Recently, AMD3100 has been shown to increase T-cell trafficking in the central nervous system, leading to significant improvement in the survival of West Nile virus encephalitis (29). Given its highly potent and selective inhibition of SDF-1–CXCR4 interaction and its bioavailability when administered orally, it is important to address whether KRH-3955 can also be used for such clinical applications.

One important issue to be addressed is whether HIV-1 strains resistant to other CXCR4 antagonists show cross-resistance to KRH-3955. In our preliminary studies, AMD3100-resistant HIV-1 (kindly provided by M. Baba, Kagoshima University) (4) showed ~19-fold resistance to KRH-3955 compared with parental NL4-3, whereas the resistant virus showed ~40-fold resistance to both AMD3100 and AMD070 in MT-4 cells (data not shown). Interestingly, the AMD3100-resistant HIV-1 strain was relatively sensitive to T22, another prototype CXCR4 antagonist. Thus, KRH-3955 target sites on CXCR4 seem to partially overlap those of AMD3100, although experiments with CXCR4 mutants do not support this idea. It is important to establish KRH-3955-resistant mutants and investigate whether they also show cross-resistance to other CXCR4 antagonists. Long-term culture experiments with PM1/CCR5 cells that express both CXCR4 and CCR5 infected with X4 HIV-1 in the presence of KRH-3955 are in progress.

In conclusion, KRH-3955 is a small-molecule antagonist of the CXCR4 receptor that is bioavailable when administered orally. The compound potently and selectively inhibits X4 HIV-1 infection both in vitro and in vivo. Thus, KRH-3955 is a promising antiviral agent for HIV-1 infection and should be evaluated for its clinical efficacy and safety in humans.

ACKNOWLEDGMENTS

We thank E. Freed for his critical review of the manuscript. We thank Y. Koyanagi, and R. Collman for generously providing plasmids and thank M. Baba for AMD3100-resistant HIV-1.

The following reagents were obtained from the NIH AIDS Research and Reference Reagent Program: saquinavir, subtype B HIV-1 primary isolates 92HT593, 92HT599 (N. Hasley), and 91US005 (B. Hahn) and AZT-resistant HIV-1 A018 (D. Richman). This work was supported in part by a grant for Research on HIV/AIDS from the Ministry of Health, Labor, and Welfare of Japan.

REFERENCES

1. **Adachi, A., H. E. Gendelman, S. Koenig, T. Folks, R. Willey, A. Rabson, and M. A. Martin.** 1986. Production of acquired immunodeficiency syndrome-associated retrovirus in human and nonhuman cells transfected with an infectious molecular clone. J. Virol. **59**:284–291.
2. **Alkhatib, G., C. Combadiere, C. C. Broder, Y. Feng, P. E. Kennedy, P. M. Murphy, and E. A. Berger.** 1996. CC CKR5: a RANTES, MIP-1α, MIP-1β receptor as a fusion cofactor for macrophage-tropic HIV-1. Science **272**:1955–1958.
3. **Amara, A., S. L. Gall, O. Schwartz, J. Salamero, M. Montes, P. Loetscher, M. Baggiolini, J. L. Virelizier, and F. Arenzana-Seisdedos.** 1997. HIV coreceptor downregulation as antiviral principle: SDF-1α-dependent internalization of the chemokine receptor CXCR4 contributes to inhibition of HIV replication. J. Exp. Med. **186**:139–146.
4. **Arakaki, R., H. Tamamura, M. Premanathan, K. Kanbara, S. Ramanan, K. Mochizuki, M. Baba, N. Fujii, and H. Nakashima.** 1999. T134, a small-molecule CXCR4 inhibitor, has no cross-drug resistance with AMD3100, a CXCR4 antagonist with a different structure. J. Virol. **73**:1719–1723.
5. **Baba, M., O. Nishimura, N. Kanzaki, M. Okamoto, H. Sawada, Y. Iizawa, M. Shiraishi, Y. Aramaki, K. Okonogi, Y. Ogawa, K. Meguro, and M. Fujino.** 1999. A small-molecule, nonpeptide CCR5 antagonist with highly potent and selective anti-HIV-1 activity. Proc. Natl. Acad. Sci. USA **96**:5698–5703.
6. **Baba, M., K. Takashima, H. Miyake, N. Kanzaki, K. Teshima, X. Wang, M. Shiraishi, and Y. Iizawa.** 2005. TAK-652 inhibits CCR5-mediated human immunodeficiency virus type 1 infection in vitro and has favorable pharmacokinetics in humans. Antimicrob. Agents Chemother. **49**:4584–4591.
7. **Bleul, C. C., M. Farzan, H. Choe, C. Parolin, I. Clark-Lewis, J. Sodroski, and T. A. Springer.** 1996. The lymphocyte chemoattractant SDF-1 is a ligand for LESTR/fusin and blocks HIV-1 entry. Nature **382**:829–833.
8. **Brelot, A., N. Heveker, M. Montes, and M. Alizon.** 2000. Identification of residues of CXCR4 critical for human immunodeficiency virus coreceptor and chemokine receptor activities. J. Biol. Chem. **275**:23736–23744.
9. **Coakley, E., C. J. Petropoulos, and J. M. Whitcomb.** 2005. Assessing chemokine co-receptor usage in HIV. Curr. Opin. Infect. Dis. **18**:9–15.
10. **Cocchi, F., A. L. DeVico, D. A. Garzino, S. K. Arya, R. C. Gallo, and P. Lusso.** 1995. Identification of RANTES, MIP-1α, and MIP-1β as the major HIV-suppressive factors produced by $CD8^+$ T cells. Science **270**:1811–1815.
11. **Collman, R., J. W. Balliet, S. A. Gregory, H. Friedman, D. L. Kolson, N. Nathanson, and A. Srinivasan.** 1992. An infectious molecular clone of an unusual macrophage-tropic and highly cytopathic strain of human immunodeficiency virus type 1. J. Virol. **66**:7517–7521.
12. **Connor, R. I., K. E. Sheridan, D. Ceradini, S. Choe, and N. R. Landau.** 1997. Change in coreceptor use correlates with disease progression in HIV-1-infected individuals. J. Exp. Med. **185**:621–628.
13. **Daar, E. S., K. L. Kesler, C. J. Petropoulos, W. Huang, M. Bates, A. E. Lail, E. P. Coakley, E. D. Gomperts, and S. M. Donfield.** 2007. Baseline HIV type 1 coreceptor tropism predicts disease progression. Clin. Infect. Dis. **45**:643–649.
14. **De Clercq, E.** 2005. Potential clinical applications of the CXCR4 antagonist bicyclam AMD3100. Mini Rev. Med. Chem. **5**:805–824.
15. **Deng, H., R. Liu, W. Ellmeier, S. Choe, D. Unutmaz, M. Burkhart, M. P. Di, S. Marmon, R. E. Sutton, C. M. Hill, C. B. Davis, S. C. Peiper, T. J. Schall, D. R. Littman, and N. R. Landau.** 1996. Identification of a major co-receptor for primary isolates of HIV-1. Nature **381**:661–666.

16. **Donzella, G. A., D. Schols, S. W. Lin, J. A. Este, K. A. Nagashima, P. J. Maddon, G. P. Allaway, T. P. Sakmar, G. Henson, E. De Clercq, and J. P. Moore.** 1998. AMD3100, a small molecule inhibitor of HIV-1 entry via the CXCR4 co-receptor. Nat. Med. **4**:72–77.
17. **Dorr, P., M. Westby, S. Dobbs, P. Griffin, B. Irvine, M. Macartney, J. Mori, G. Rickett, C. Smith-Burchnell, C. Napier, R. Webster, D. Armour, D. Price, B. Stammen, A. Wood, and M. Perros.** 2005. Maraviroc (UK-427,857), a potent, orally bioavailable, and selective small-molecule inhibitor of chemokine receptor CCR5 with broad-spectrum anti-human immunodeficiency virus type 1 activity. Antimicrob. Agents Chemother. **49**:4721–4732.
18. **Dragic, T., V. Litwin, G. P. Allaway, S. R. Martin, Y. Huang, K. A. Nagashima, C. Cayanan, P. J. Maddon, R. A. Koup, J. P. Moore, and W. A. Paxton.** 1996. HIV-1 entry into CD4$^+$ cells is mediated by the chemokine receptor CC-CKR-5. Nature **381**:667–673.
19. **Feng, Y., C. C. Broder, P. E. Kennedy, and E. A. Berger.** 1996. HIV-1 entry cofactor: functional cDNA cloning of a seven-transmembrane, G protein-coupled receptor. Science **272**:872–877.
20. **Gerlach, L. O., R. T. Skerlj, G. J. Bridger, and T. W. Schwartz.** 2001. Molecular interactions of cyclam and bicyclam non-peptide antagonists with the CXCR4 chemokine receptor. J. Biol. Chem. **276**:14153–14160.
21. **Hendrix, C. W., A. C. Collier, M. M. Lederman, D. Schols, R. B. Pollard, S. Brown, J. B. Jackson, R. W. Coombs, M. J. Glesby, C. W. Flexner, G. J. Bridger, K. Badel, R. T. MacFarland, G. W. Henson, and G. Calandra.** 2004. Safety, pharmacokinetics, and antiviral activity of AMD3100, a selective CXCR4 receptor inhibitor, in HIV-1 infection. J. Acquir. Immune Defic. Syndr. **37**:1253–1262.
22. **Hendrix, C. W., C. Flexner, R. T. MacFarland, C. Giandomenico, E. J. Fuchs, E. Redpath, G. Bridger, and G. W. Henson.** 2000. Pharmacokinetics and safety of AMD-3100, a novel antagonist of the CXCR-4 chemokine receptor, in human volunteers. Antimicrob. Agents Chemother. **44**:1667–1673.
23. **Ichiyama, K., S. Yokoyama-Kumakura, Y. Tanaka, R. Tanaka, K. Hirose, K. Bannai, T. Edamatsu, M. Yanaka, Y. Niitani, N. Miyano-Kurosaki, H. Takaku, Y. Koyanagi, and N. Yamamoto.** 2003. A duodenally absorbable CXC chemokine receptor 4 antagonist, KRH-1636, exhibits a potent and selective anti-HIV-1 activity. Proc. Natl. Acad. Sci. USA **100**:4185–4190.
24. **Kikukawa, R., Y. Koyanagi, S. Harada, N. Kobayashi, M. Hatanaka, and N. Yamamoto.** 1986. Differential susceptibility to the acquired immunodeficiency syndrome retrovirus in cloned cells of human leukemic T-cell line Molt-4. J. Virol. **57**:1159–1162.
25. **Koyanagi, Y., S. Miles, R. T. Mitsuyasu, J. E. Merrill, H. V. Vinters, and I. S. Chen.** 1987. Dual infection of the central nervous system by AIDS viruses with distinct cellular tropisms. Science **236**:819–822.
26. **Larder, B. A., G. Darby, and D. D. Richman.** 1989. HIV with reduced sensitivity to zidovudine (AZT) isolated during prolonged therapy. Science **243**:1731–1734.
27. **Liu, R., W. A. Paxton, S. Choe, D. Ceradini, S. R. Martin, R. Horuk, M. E. MacDonald, H. Stuhlmann, R. A. Koup, and N. R. Landau.** 1996. Homozygous defect in HIV-1 coreceptor accounts for resistance of some multiply-exposed individuals to HIV-1 infection. Cell **86**:367–377.
28. **Maeda, K., H. Nakata, Y. Koh, T. Miyakawa, H. Ogata, Y. Takaoka, S. Shibayama, K. Sagawa, D. Fukushima, J. Moravek, Y. Koyanagi, and H. Mitsuya.** 2004. Spirodiketopiperazine-based CCR5 inhibitor which preserves CC-chemokine/CCR5 interactions and exerts potent activity against R5 human immunodeficiency virus type 1 in vitro. J. Virol. **78**:8654–8662.
29. **McCandless, E. E., B. Zhang, M. S. Diamond, and R. S. Klein.** 2008. CXCR4 antagonism increases T cell trafficking in the central nervous system and improves survival from West Nile virus encephalitis. Proc. Natl. Acad. Sci. USA **105**:11270–11275.
30. **Murakami, T., T. Nakajima, Y. Koyanagi, K. Tachibana, N. Fujii, H. Tamamura, N. Yoshida, M. Waki, A. Matsumoto, O. Yoshie, T. Kishimoto, N. Yamamoto, and T. Nagasawa.** 1997. A small molecule CXCR4 inhibitor that blocks T cell line-tropic HIV-1 infection. J. Exp. Med. **186**:1389–1393.
31. **Murakami, T., T. Y. Zhang, Y. Koyanagi, Y. Tanaka, J. Kim, Y. Suzuki, S. Minoguchi, H. Tamamura, M. Waki, A. Matsumoto, N. Fujii, H. Shida, J. A. Hoxie, S. C. Peiper, and N. Yamamoto.** 1999. Inhibitory mechanism of the CXCR4 antagonist T22 against human immunodeficiency virus type 1 infection. J. Virol. **73**:7489–7496.
32. **Nagasawa, T., S. Hirota, K. Tachibana, N. Takakura, S. Nishikawa, Y. Kitamura, N. Yoshida, H. Kikutani, and T. Kishimoto.** 1996. Defects of B-cell lymphopoiesis and bone-marrow myelopoiesis in mice lacking the CXC chemokine PBSF/SDF-1. Nature **382**:635–638.
33. **Nakashima, H., M. Masuda, T. Murakami, Y. Koyanagi, A. Matsumoto, N. Fujii, and N. Yamamoto.** 1992. Anti-human immunodeficiency virus activity of a novel synthetic peptide, T22 ([Tyr-5,12, Lys-7]polyphemusin II): a possible inhibitor of virus-cell fusion. Antimicrob. Agents Chemother. **36**:1249–1255.
34. **Oberlin, E., A. Amara, F. Bachelerie, C. Bessia, J. L. Virelizier, F. Arenzana-Seisdedos, O. Schwartz, J. M. Heard, I. Clark-Lewis, D. F. Legler, M. Loetscher, M. Baggiolini, and B. Moser.** 1996. The CXC chemokine SDF-1 is the ligand for LESTR/fusin and prevents infection by T-cell-line-adapted HIV-1. Nature **382**:833–835.
35. **Richman, D. D., and S. A. Bozzette.** 1994. The impact of the syncytium-inducing phenotype of human immunodeficiency virus on disease progression. J. Infect. Dis. **169**:968–974.
36. **Roehm, N. W., G. H. Rodgers, S. M. Hatfield, and A. L. Glasebrook.** 1991. An improved colorimetric assay for cell proliferation and viability utilizing the tetrazolium salt XTT. J. Immunol. Methods **142**:257–265.
37. **Rosenkilde, M. M., L. O. Gerlach, S. Hatse, R. T. Skerlj, D. Schols, G. J. Bridger, and T. W. Schwartz.** 2007. Molecular mechanism of action of monocyclam versus bicyclam non-peptide antagonists in the CXCR4 chemokine receptor. J. Biol. Chem. **282**:27354–27365.
38. **Rosenkilde, M. M., L. O. Gerlach, J. S. Jakobsen, R. T. Skerlj, G. J. Bridger, and T. W. Schwartz.** 2004. Molecular mechanism of AMD3100 antagonism in the CXCR4 receptor: transfer of binding site to the CXCR3 receptor. J. Biol. Chem. **279**:3033–3041.
39. **Samson, M., F. Libert, B. J. Doranz, J. Rucker, C. Liesnard, C. M. Farber, S. Saragosti, C. Lapoumeroulie, J. Cognaux, C. Forceille, G. Muyldermans, C. Verhofstede, G. Burtonboy, M. Georges, T. Imai, S. Rana, Y. Yi, R. J. Smyth, R. G. Collman, R. W. Doms, G. Vassart, and M. Parmentier.** 1996. Resistance to HIV-1 infection in Caucasian individuals bearing mutant alleles of the CCR-5 chemokine receptor gene. Nature **382**:722–725.
40. **Schols, D., S. Struyf, J. Van Damme, J. A. Este, G. Henson, and E. De Clercq.** 1997. Inhibition of T-tropic HIV strains by selective antagonization of the chemokine receptor CXCR4. J. Exp. Med. **186**:1383–1388.
41. **Stone, N. D., S. B. Dunaway, C. Flexner, C. Tierney, G. B. Calandra, S. Becker, Y. J. Cao, I. P. Wiggins, J. Conley, R. T. MacFarland, J. G. Park, C. Lalama, S. Snyder, B. Kallungal, K. L. Klingman, and C. W. Hendrix.** 2007. Multiple-dose escalation study of the safety, pharmacokinetics, and biologic activity of oral AMD070, a selective CXCR4 receptor inhibitor, in human subjects. Antimicrob. Agents Chemother. **51**:2351–2358.
42. **Strizki, J. M., C. Tremblay, S. Xu, L. Wojcik, N. Wagner, W. Gonsiorek, R. W. Hipkin, C. C. Chou, C. Pugliese-Sivo, Y. Xiao, J. R. Tagat, K. Cox, T. Priestley, S. Sorota, W. Huang, M. Hirsch, G. R. Reyes, and B. M. Baroudy.** 2005. Discovery and characterization of vicriviroc (SCH 417690), a CCR5 antagonist with potent activity against human immunodeficiency virus type 1. Antimicrob. Agents Chemother. **49**:4911–4919.
43. **Strizki, J. M., S. Xu, N. E. Wagner, L. Wojcik, J. Liu, Y. Hou, M. Endres, A. Palani, S. Shapiro, J. W. Clader, W. J. Greenlee, J. R. Tagat, S. McCombie, K. Cox, A. B. Fawzi, C. C. Chou, C. Pugliese-Sivo, L. Davies, M. E. Moreno, D. D. Ho, A. Trkola, C. A. Stoddart, J. P. Moore, G. R. Reyes, and B. M. Baroudy.** 2001. SCH-C (SCH 351125), an orally bioavailable, small molecule antagonist of the chemokine receptor CCR5, is a potent inhibitor of HIV-1 infection in vitro and in vivo. Proc. Natl. Acad. Sci. USA **98**:12718–12723.
44. **Tachibana, K., S. Hirota, H. Iizasa, H. Yoshida, K. Kawabata, Y. Kataoka, Y. Kitamura, K. Matsushima, N. Yoshida, S. Nishikawa, T. Kishimoto, and T. Nagasawa.** 1998. The chemokine receptor CXCR4 is essential for vascularization of the gastrointestinal tract. Nature **393**:591–594.
45. **Takashima, K., H. Miyake, N. Kanzaki, Y. Tagawa, X. Wang, Y. Sugihara, Y. Iizawa, and M. Baba.** 2005. Highly potent inhibition of human immunodeficiency virus type 1 replication by TAK-220, an orally bioavailable small-molecule CCR5 antagonist. Antimicrob. Agents Chemother. **49**:3474–3482.
46. **Tamamura, H., H. Tsutsumi, H. Masuno, and N. Fujii.** 2007. Development of low molecular weight CXCR4 antagonists by exploratory structural tuning of cyclic tetra- and pentapeptide-scaffolds towards the treatment of HIV infection, cancer metastasis and rheumatoid arthritis. Curr. Med. Chem. **14**:93–102.
47. **Tanaka, R., A. Yoshida, T. Murakami, E. Baba, J. Lichtenfeld, T. Omori, T. Kimura, N. Tsurutani, N. Fujii, Z. X. Wang, S. C. Peiper, N. Yamamoto, and Y. Tanaka.** 2001. Unique monoclonal antibody recognizing the third extracellular loop of CXCR4 induces lymphocyte agglutination and enhances human immunodeficiency virus type 1-mediated syncytium formation and productive infection. J. Virol. **75**:11534–11543.
48. **Urano, E., T. Aoki, Y. Futahashi, T. Murakami, Y. Morikawa, N. Yamamoto, and J. Komano.** 2008. Substitution of the myristoylation signal of human immunodeficiency virus type 1 $Pr55^{Gag}$ with the phospholipase C-δ1 pleckstrin homology domain results in infectious pseudovirion production. J. Gen. Virol. **89**:3144–3149.
49. **Westby, M., M. Lewis, J. Whitcomb, M. Youle, A. L. Pozniak, I. T. James, T. M. Jenkins, M. Perros, and E. van der Ryst.** 2006. Emergence of CXCR4-using human immunodeficiency virus type 1 (HIV-1) variants in a minority of HIV-1-infected patients following treatment with the CCR5 antagonist maraviroc is from a pretreatment CXCR4-using virus reservoir. J. Virol. **80**:4909–4920.
50. **Xiao, L., D. L. Rudolph, S. M. Owen, T. J. Spira, and R. B. Lal.** 1998. Adaptation to promiscuous usage of CC and CXC-chemokine coreceptors in vivo correlates with HIV-1 disease progression. AIDS **12**:F137–F143.
51. **Yoshida, A., R. Tanaka, T. Murakami, Y. Takahashi, Y. Koyanagi, M. Nakamura, M. Ito, N. Yamamoto, and Y. Tanaka.** 2003. Induction of protective immune responses against R5 human immunodeficiency virus type 1 (HIV-1) infection in hu-PBL–SCID mice by intrasplenic immunization with HIV-1-pulsed dendritic cells: possible involvement of a novel factor of human CD4$^+$ T-cell origin. J. Virol. **77**:8719–8728.
52. **Zou, Y. R., A. H. Kottmann, M. Kuroda, I. Taniuchi, and D. R. Littman.** 1998. Function of the chemokine receptor CXCR4 in haematopoiesis and in cerebellar development. Nature **393**:595–599.

Journal of Cellular Physiology

Dys-Regulated Activation of a Src Tyroine Kinase Hck at the Golgi Disturbs *N*-Glycosylation of a Cytokine Receptor Fms

RANYA HASSAN,[1] SHINYA SUZU,[1] MASATERU HIYOSHI,[1] NAOKO TAKAHASHI-MAKISE,[1] TAKAMASA UENO,[2] TSUTOMU AGATSUMA,[3] HIROFUMI AKARI,[4] JUN KOMANO,[5] YUTAKA TAKEBE,[6] KAZUO MOTOYOSHI,[7] AND SEIJI OKADA[1]*

[1]*Division of Hematopoiesis, Center for AIDS Research, Kumamoto University, Kumamoto, Kumamoto, Japan*

[2]*Viral Immunology, Center for AIDS Research, Kumamoto University, Kumamoto, Kumamoto, Japan*

[3]*Tokyo Research Laboratories, Kyowa Hakko Co., Ltd, Machida, Tokyo, Japan*

[4]*Laboratory of Disease Control, Tsukuba Primate Research Center, National Institute of Biomedical Innovation, Tsukuba, Ibaraki, Japan*

[5]*Laboratory of Virology and Pathogenesis, AIDS Research Center, National Institute of Infectious Diseases, Shinjuku, Tokyo, Japan*

[6]*Laboratory of Molecular Biology and Epidemiology, AIDS Research Center, National Institute of Infectious Diseases, Shinjuku, Tokyo, Japan*

[7]*Department of Internal Medicine, National Defense Medical College, Tokorozawa, Saitama, Japan*

HIV-1 Nef accelerates the progression to AIDS by binding with and activating a Src kinase Hck, but underlying molecular basis is not understood. We revealed that Nef disturbed *N*-glycosylation/trafficking of a cytokine receptor Fms in an Hck-dependent manner, a possible trigger to worsen uncontrolled immune system. Here, we provide direct evidence that dys-regulated activation of Hck pre-localized to the Golgi apparatus causes this Fms maturation arrest. A striking change in Hck induced by Nef other than activation was its skewed localization to the Golgi due to predominant Golgi-localization of Nef. Studies with different Nef alleles and their mutants showed a clear correlation among higher Nef-Hck affinity, stronger Hck activation, severe Golgi-localization of Hck and severe Fms maturation arrest. Studies with a newly discovered Nef-Hck binding blocker 2c more clearly showed that skewed Golgi-localization of active Hck was indeed the cause of Fms maturation arrest. 2c blocked Nef-induced skewed Golgi-localization of an active form of Hck (Hck-P2A) and Fms maturation arrest by Nef/Hck-P2A, but showed no inhibition on Hck-P2A kinase activity. Our finding establishes an intriguing link between the pathogenesis of Nef and a newly emerging concept that the Golgi-localized Src kinases regulate the Golgi function.

J. Cell. Physiol. 221: 458–468, 2009.

Studies of HIV-1-infected patients and monkey models have demonstrated that Nef, a protein with no enzymatic activity encoded by the HIV-1 genome, is a critical determinant for the development of AIDS (Kestler et al., 1991; Deacon et al., 1995; Kirchhoff et al., 1995). Subsequent studies of HIV-1 transgenic (Tg) mice supported the idea. The expression of entire coding sequences of HIV-1 in $CD4^+$ T cells and macrophages caused an AIDS-like disease, which was abolished by Nef deletion (Hanna et al., 1998). This pathogenetic activity of Nef is supposed to be mediated by its binding with cellular proteins, and a well-defined partner of Nef is Hck (Saksela et al., 1995), a member of Src family tyrosine kinases expressed in macrophages. Other Src kinases (Lyn, Fyn, c-Src, and Lck) bind Nef but with lower affinities (Arold et al., 1998; Karkkainen et al., 2006; Trible et al., 2006). Importantly, the disruption of proline-rich PxxP motif of Nef, an essential motif to bind the Src homology 3 (SH3) domain of Hck, was sufficient to protect Tg mice from the AIDS-like disease, and wild-type Nef-induced disease progression was significantly delayed in $Hck^{-/-}$ mice (Hanna et al., 2001), indicating that high affinity Nef-Hck binding in macrophages is at least in part responsible for disease development and progression. However, unresolved issue is how Nef-Hck binding followed by activation of Hck (Moarefi et al., 1997; Lerner and Smithgall, 2002) satisfactorily account for disease development and progression.

An important clue to the issue is that Nef predominantly localized to the Golgi apparatus (Greenberg et al., 1998; Drakesmith et al., 2005; Haller et al., 2007) and that Nef not only activated Hck but also induced skewed localization of Hck to the Golgi (Hung et al., 2007). The Golgi functions as a sorting hub and location of glycosylation for proteins, and several lines of evidence have revealed that Src kinases, shown to be involved in a wide array of intracellular signaling (reviewed in

Contract grant sponsor: Ministry of Education, Culture, Sports, Science and Technology of Japan.
Contract grant sponsor: Human Science Foundation, Japan.

*Correspondence to: Seiji Okada, Division of Hematopoiesis, Center for AIDS Research, Kumamoto University, Kumamoto 860-0811, Japan. E-mail: okadas@kumamoto-u.ac.jp

Received 17 February 2009; Accepted 11 June 2009

Published online in Wiley InterScience (www.interscience.wiley.com.), 7 July 2009.
DOI: 10.1002/jcp.21878

Lowell, 2004), also play a role in the regulation of the Golgi structure/function. First, a fraction of Src kinases, including Hck, is physiologically found at the Golgi (David-Pfeuty and Nouvian-Dooghe, 1990; Kaplan et al., 1992; Ley et al., 1994; Bijlmakers et al., 1997; van't Hof and Resh, 1997; Carreno et al., 2000; Kasahara et al., 2004). Second, fibroblasts lacking three ubiquitous Src kinases (c-Src/Yes/Fyn) exhibited an aberrant Golgi structure composed of collapsed stacks and bloated cisternae (Bard et al., 2003). Third, an increased protein load entering the *cis*-Golgi from the endoplasmic reticulum activated the Golgi-localized Src kinases, which in turn regulated overall protein trafficking activity in the secretory pathway (Pulvirenti et al., 2008). Importantly, the study by Pulvirenti et al. indicates that coordinated regulation of activity of the Golgi-localized Src kinases is crucial to maintain the Golgi function, which raises an intriguing possibility that Nef affects protein trafficking process and thereby macrophage phenotype/function through skewed Golgi-localization of active Hck.

Indeed, we recently identified an aberrant function of Nef, which was possibly due to the skewed Golgi-localization of active Hck. We previously found that Nef inhibited the signal of M-CSF, a primary cytokine for macrophages (Suzu et al., 2005), which was a possible trigger to worsen uncontrolled immune systems in patients, as M-CSF is essential to maintain macrophages at an anti-inflammatory state (reviewed in Hamilton, 2008). Of interest was the role of Hck in this inhibitory activity of Nef (Hiyoshi et al., 2008). Nef reduced cell surface expression of M-CSF receptor Fms in myeloid cells and macrophages, which was the direct cause of the inhibitory activity of Nef on M-CSF signal. Importantly, such reduced cell surface expression of Fms was reproduced in transfected 293 cells, but only in co-expression with Hck. More importantly, the reduced cell surface expression was due to the accumulation of an immature under-*N*-glycosylated Fms at the Golgi (hereinafter called Fms maturation arrest). However, constitutive-active Hck alone failed to induce such Fms maturation arrest. These results indicate that Nef inhibits M-CSF signal by arresting Fms *N*-glycosylation and trafficking at the Golgi and that such Fms maturation arrest was not caused just because of Hck activation. Thus, a most likely cause of Nef-induced Fms maturation arrest was skewed Golgi-localization of active Hck. However, this intriguing hypothesis should be carefully and directly tested, because it will not only help to clarify molecular basis of this novel function of Nef through Hck, but also provide an excellent example of disease-associated failure of the Golgi function regulation by the Golgi-localized Src kinases.

In this study, we therefore sought to definitely conclude that skewed Golgi-localization of active Hck was indeed the direct cause of Fms maturation arrest by Nef. To this end, we employed two different approaches. First, we prepared various Nef proteins and compared their abilities to induce skewed Golgi-localization of Hck, Hck activation and Fms maturation arrest. Second and importantly, we discovered a small-molecule non-kinase inhibitor that effectively blocked Nef-Hck binding and performed mechanistic analyses with the newly discovered compound.

Materials and Methods

Expression plasmids

For the expression in HEK293 cells (Invitrogen, Carlsbad, CA), human Fms- and human p56Hck cDNA cloned into pCDNA3.1 vector (Invitrogen) were used (Suzu et al., 2005; Hiyoshi et al., 2008). The constitutive-active Hck P2A mutant (Hiyoshi et al., 2008) was also used in selected experiments. The expression plasmid for human Lyn cloned in pME-puro vector was provided by Y. Yamanashi (Tokyo Medical and Dental University, Tokyo, Japan) and used in the pull-down assay with GST-Nef fusion proteins (see below). Nef cDNA derived from the NL43 or SF2 strain of HIV-1 was cloned into pRc/CMV-CD8 vector to express the extracellular/transmembrane regions of CD8-Nef fusion protein (Hiyoshi et al., 2008). NL43 Nef-M20A was prepared as described previously (Akari et al., 2000). NL43 Nef-AxxA and −ΔE mutant were provided by A. Adachi (University of Tokushima, Tokushima, Japan) and J.C. Guatelli (University of California, San Diego, CA), respectively. In this study, we prepared another NL43 Nef mutant (NL43 Nef-TR), by using QuikChange II Site-directed Mutagenesis Kits (Stratagene, La Jolla, CA). We also prepared Nef constructs expressing Nef-GFP fusion proteins (Ueno et al., 2008). For the expression of GST-Nef fusion proteins, fragments containing the entire coding sequences of the wild-type NL43 Nef, NL43 Nef-TR mutant, wild-type SF2 Nef, and SF2 Nef-AxxA mutant were subcloned into pGEX-6P-1 vector (GE Healthcare, Buckinghamshire, UK). SF2 Nef-AxxA mutant was prepared by using QuikChange II Site-directed Mutagenesis Kits (Stratagene). The nucleotide sequences of the coding region of all Nef constructs were verified by using BigDye Terminator v3.1 Cycle Sequencing Kit (Applied Biosystems, Foster City, CA) and ABI PRISM 3100 Genetic Analyzer (Applied Biosystems).

Chemicals

PP2 (Sigma, San Diego, CA) was used as the Src kinase inhibitor. UCS15A and its synthetic derivatives, 2b and 2c, were prepared as described (Oneyama et al., 2003). All these inhibitors were dissolved in dimethyl sulfoxide (DMSO; Wako, Osaka, Japan).

Western blotting

HEK293 cells were maintained with DME medium (Wako) supplemented with 10% fetal calf serum (FCS). The maturation of Fms proteins or the activation of Hck was analyzed by the transient expression assay with the cells followed by Western blotting as described previously (Suzu et al., 2005; Hiyoshi et al., 2008). In brief, cells grown on a 12-well tissue culture plate were transfected with plasmid for Fms (0.4 μg), Nef (0.8 μg), or Hck (0.4 μg) in the combinations indicated using LipofectAMINE2000 reagent (Invitrogen), unless otherwise stated. Total amounts of plasmids were normalized with the empty vectors. After 6 h, culture medium was replaced with complete medium and the transfected cells were cultured for an additional 42 h. In selected experiments, chemicals such as PP2 and 2c were added to the culture at the same time of changing medium. Total cell lysates were prepared essentially as described (Suzu et al., 2000). Primary antibodies used for Western blotting were as follows: anti-Fms (C-20; Santa Cruz Biotechnology, Santa Cruz, CA), anti-CD8 (H-160; Santa Cruz), anti-GFP (FL; Santa Cruz), anti-Hck (clone 18; Transduction Laboratories, Lexington, KY), anti-Hck phosphorylated at tyrosine 411 (Hck-pTyr^{411}; Santa Cruz), anti-phosphotyrosine (PY99; Santa Cruz), and anti-ERK1/2 (K-23; Santa Cruz). The relative intensity of bands on scanned gel images was quantified using NIH Image software, and the Fms maturation arrest or Hck activation is also shown graphically on an arbitrary unit. The relative intensity of bands on Hck-pTyr^{411} blots was quantified and the degree of Hck activation was expressed as a fold-increase relative to the control. For Fms maturation arrest, we calculated the percentage of immature under-*N*-glycosylated Fms of total Fms protein amount, and compared the percentages among samples.

Immunofluorescence

The signal of Nef-GFP was directly visualized with a BZ-8000 fluorescent microscope (Keyence, Osaka, Japan) equipped with Plan-Fluor ELWD 20x/0.45 objective lenses (Nikon, Tokyo, Japan) (Hiyoshi et al., 2008). To detect active Hck, cells were fixed in 2% paraformaldehyde, permeabilized with ethanol, and stained with goat anti-active Hck antibodies (Santa Cruz). Secondary antibodies were anti-goat IgG-AlexaFluo488 (Molecular Probes, Eugene, OR). Nuclei were stained with DAPI (Molecular Probes), and

fluorescent signals were visualized as above. Image processing was performed using BZ-analyzer (Keyence) and Adobe Photoshop Software (Adobe Systems, San Jose, CA).

GST pull-down

The control GST or GST-Nef fusion proteins (wild-type NL43 Nef, NL43 Nef-TR, wild-type SF2 Nef, and SF2 Nef-AxxA) cloned in pGEX-6P-1 vector was expressed in *E. coli* BL21 cells (GE Healthcare). Cells were grown in LB media containing 50 μg/ml ampicillin followed by induction with 1 μM IPTG. The expression-induced cells were harvested and lysed with BugBuster Protein Extraction Reagent containing 1 U/ml rLysozyme and 25 U/ml Benzonaze Nuclease (Novagen, Madison, WI). The cleared lysates were then incubated with GST-Bind Resin (Novagen). After extensive washing with GST Bind/Wash Buffer (Novagen), the resin was incubated with the total cell lysates of HEK293 cells transfected with the expression plasmid for Hck or Lyn. In a selected experiment, 2c was added to the mixtures. After extensive re-washing, the resin was boiled with SDS–PAGE sample buffer and elutes were analyzed for the presence of Hck or Lyn by western blotting. Primary antibodies used were as follows (both from Transduction Laboratories): anti-Hck (clone 18) and anti-Lyn (clone 42). In a selected experiment, we also used GST proteins fused to the SH3 domain of Hck (Paliwal et al., 2007), which was provided by G. Swarup (Center for Cellular and Molecular Biology, Hyderabad, India).

Subcellular fractionation

The subcellular fractionation on sucrose gradients was performed exactly as reported (Matsuda et al., 2006). In brief, cells were

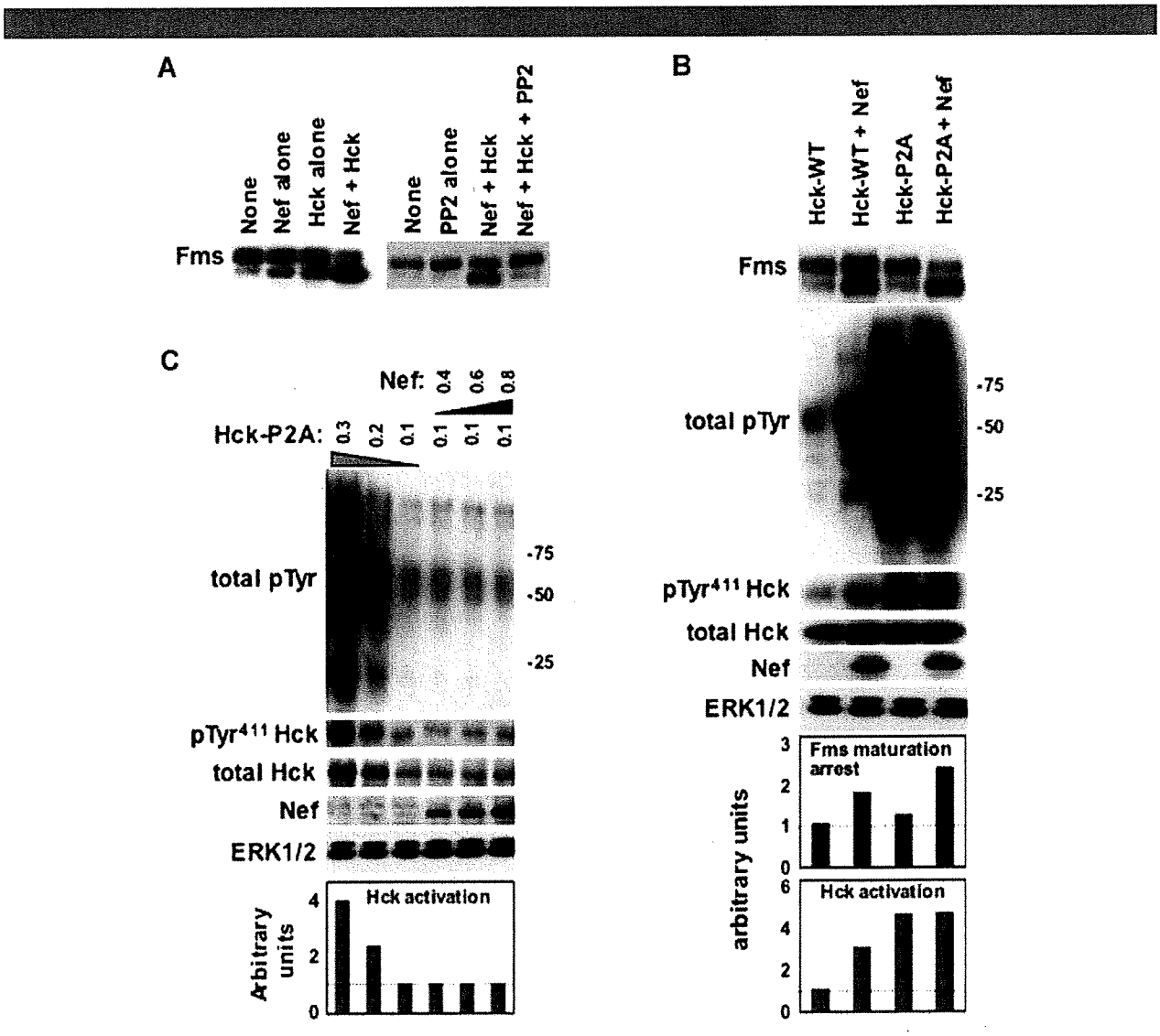

Fig. 1. Nef/Hck-induced Fms mturation arrest. A: HEK293 cells were transfected with Fms plamid alone (None) or co-transfected with the plasmids for NL43 Nef and/or wild-type Hck as indicated. In the right blot, PP2 was added to selected wells at a final concentration of 10 μM after the transfection, Total cell lysates were subjected to Fms Western blotting. B: Cells were transfected with Fms plasmid alone (None) or in combination with the plasmids for Nef (NL43) and Hck (WT or constitutive-active P2A), as indicated. These cells were then analyzed for the expression of Fms, tyrosine-phosphorylated proteins (total pTyr), active-Hck (pTyr^{411}Hck), total Hck, CD8-Nef (Nef), or ERK by Western blotting. The ERK blot is a loading control. The quantified Fms maturation arrest and Hck activation are shown in the bar graphs. C: Cells were transfected with varying amounts (μg) of Hck-P2A and NL43 Nef plasmids as indicated, and analyzed as in (B). The quantified Hck activation is shown in the bar graphs. [Color figure can be viewed in the online issue, which is available at www.interscience.wiley.com.]